

Versatile Bandpass Filters with Wide Frequency Tunability Part II

Version 1.1

James A Crawford

Synopsis

Classical LC filter design is becoming increasingly rare in much of the RF design community. This is in part due to the domination of direct-conversion in up- and down-converters and the widespread availability of excellent off-the-shelf filter components (e.g., SAW filters).

Whether the occasion be discrete design or on-chip integrated design, the need for tunable bandpass filters still arises, however. In Part I of this article, single-pole bandpass filter design was considered for situations where passband flatness is not overly demanding but insertion loss may be a critical requirement. Part II of this article looks at the design of 2nd-order tunable bandpass filters which may prove indispensable in some circumstances.

For those readers more interested in design results rather than the theoretical background development, §6 provides several design examples and the MATLAB script used to do the design calculations is provided in §9.

1 Introduction

The primary motivations for considering the first-order bandpass filters in Part I of this material were simplicity and low insertion loss. Several lessons learned with the 1st-order filters are undoubtedly applicable to the 2nd order filter case as well. Second-order filters offer the possibility of wider passbands with much better amplitude flatness.

Lesson #1 from Part I was that the filter's internal resistance level can be crafted in a fairly flexible manner in order to realize a range of filter bandwidth versus center frequency behaviors. Lesson #2 was that the use of purely series resonators can exacerbate the insertion loss problem if FET or PIN diode switches are used to switch in different capacitance values. This is because the filter's impedance level in those resonators is fairly low compared to the on-resistance of these switching devices. Parallel resonators are therefore more advantageous for lower insertion loss since these are typically used with an internal filter impedance $R_{internal}$ greater than the port impedances R_{source} and R_{load} .

Pole and zero placement for a filter determine all of the behavior characteristics of the filter. It is generally desirable to have an equal number of transmission zeros at dc and infinity so that the lower and upper stopband behaviors can be made roughly the same. A representative filter to aid in this discussion is shown in Figure 1. In order to determine the number of transmission zeros at dc in Figure 1, it is helpful to think of each capacitor being replaced by an open-circuit and each inductor being replaced by a short-circuit as shown in Figure 2. In the portion denoted as *Cut 1*, in a resistive divider sense, an impedance open (from C_2) is working against an impedance short (from L_1) thereby contributing two transmission zeros¹. In the portion denoted as *Cut 2*, an impedance open (from C_3) is working against a non-zero impedance R_{load} so this adds only one transmission zero. The filter consequently has three transmission zeros at dc. In the case of transmission zeros at ∞ , each capacitor is replaced by a short-circuit and each inductor is replaced by an open-circuit as shown in Figure 3. For *Cut 3*, a short (from C_1) is working against a non-zero impedance R_{source} thereby contributing one transmission zero. For *Cut 4*, an open-circuit (from L_2) is working against a short-circuit (from C_4) thereby contributing two transmission zeros. The filter consequently exhibits three transmission zeros at infinite frequency making for an equal number of transmission zeros in the lower and upper stopbands as desired.

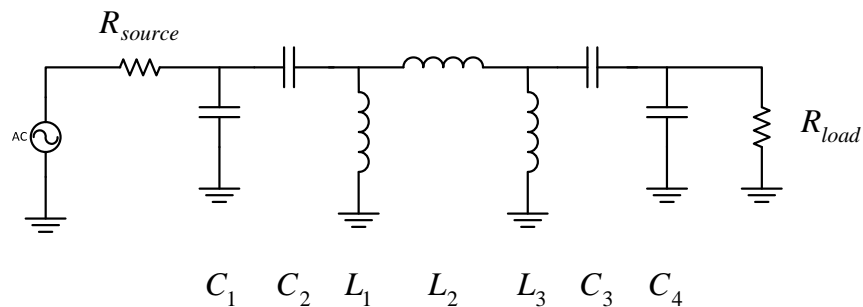


Figure 1 Representative 2nd order bandpass filter

¹ Note that parallel open-circuits count as simply one open-circuit, and parallel short-circuits count as a single short-circuit. The converse is true with series open- and short-circuits.

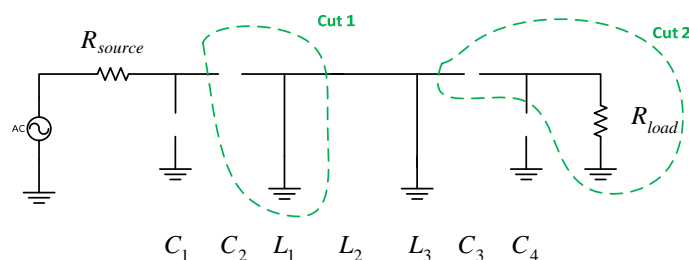


Figure 2 Bandpass filter shown in Figure 1 with impedance considerations at DC shown

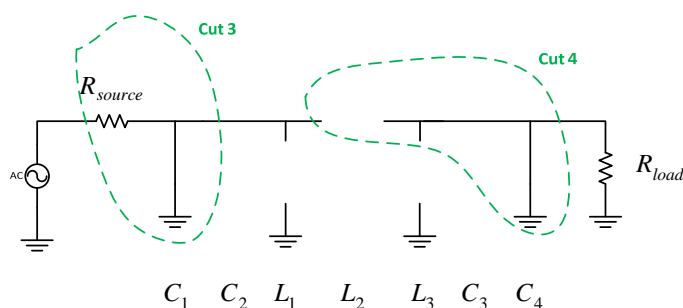


Figure 3 Bandpass filter shown in Figure 1 with impedance considerations at ∞ frequency shown

Of the 2nd-order filter topology configurations shown in Table 1, having roughly equal numbers of transmission zeros at dc and ∞ helps assure good overall stopband performance as just explained. This criterion favors configurations 2 and 4. Both topologies use parallel resonators so that is not a discriminating factor. Configuration 2 is the more interesting of the two, however, because it permits $R_{internal}$ to be larger than the port impedances whereas Configuration 4 is just the opposite. The design details behind both configurations are developed in this paper.

1.1 Some History

One of the most intriguing filter design books I happened upon early in my engineering career was the book by Daniels [1]. This book gave me a very early appreciation for filter pole/zero placement and was the primary motivation for thinking about the 2nd-order filter design problem in the context of Table 1 in the first place.

In order to make a filter tunable, inductors and or capacitors must of course be tunable. Since tunable inductors are rather intractable for traditional LC filters, the tuning elements are usually limited to capacitors. Since inductors also tend to be more lossy and larger than capacitors, it is desirable to minimize the number of inductors used; nothing new under the sun here.

I first investigated this type of tunable 2nd-order bandpass filter in connection with an SBIR project [2]. Two circuit sketches from that report making use of this filter type are shown in Figure 4 and Figure 5. Both figures make use of inductive-coupling between the two resonators based upon the tee-to-pi transformation given in §8. Note that inductive impedance transformations were used at the input and output of the filter rather than capacitive transformers as used in Configuration 2 of Table 1.

The notion of admittance and impedance inverters is also not new [3, 4, 5]. They were also used in [2] as the basis for Figure 4 and Figure 5. The inverter concept is introduced in §2 as the basis for bandpass filter design.

Table 1 Several of the Many Possible 2nd-order Bandpass Filter Alternatives²

Config #	Input Match	Resonator Coupling	Output Match	Zeros ³ @ DC	Zeros @ ∞	Schematic
1	Tapped-C	C	Tapped-C	5	1	<p style="text-align: center;">$C_1 \ C_2 \ L_1 \ C_3 \ L_2 \ C_4 \ C_5$</p>
2*	Tapped-C	L	Tapped-C	3	3	<p style="text-align: center;">$C_1 \ C_2 \ L_1 \ L_2 \ L_3 \ C_3 \ C_4$</p>
3	HPF	C	HPF	5	1	<p style="text-align: center;">$C_1 \ L_1 \ C_2 \ C_3 \ C_4 \ L_2 \ C_5$</p>
4*	HPF	L	HPF	3	3	<p style="text-align: center;">$C_1 \ L_1 \ C_2 \ L_2 \ C_3 \ L_3 \ C_4$</p>
5	LPF	C	HPF	4	2	<p style="text-align: center;">$L_1 \ C_1 \ L_2 \ C_2 \ L_3 \ C_3 \ C_4$</p>
6	LPF	L	HPF	2	4	<p style="text-align: center;">$L_1 \ C_1 \ L_2 \ L_3 \ L_4 \ C_2 \ C_3$</p>

² Configurations 2 and 4 are preferred. Schematics from U22437 Figures for U22436.vsd.

³ Transmission zeros at DC and infinity provide an indication about the lower and upper stopband behaviors.

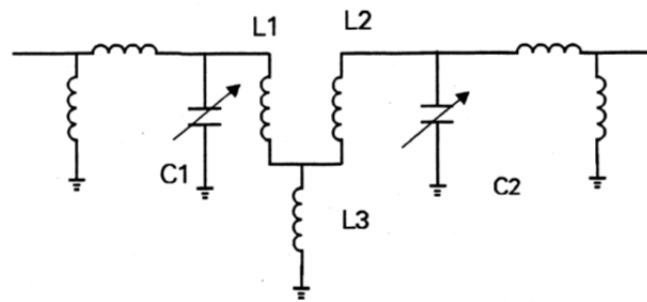


Figure 4 2nd-order tunable bandpass filter from [2] using inductive-tee coupling

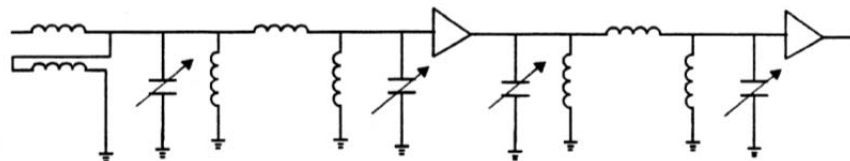


Figure 5 2nd-order tunable bandpass filter from [2] using inductive-pi coupling

1.2 Outline for the Paper

The paper is organized into four main sections:

Section I: The core of the filter based upon admittance and impedance inverters is developed while postponing discussions about the input/output sections (e.g., capacitors C_1 , C_2 , C_3 , and C_4 in configuration #2 of Table 1). This material will likely be familiar for some readers.

Section II: This portion of the paper is focused upon the input/output sections which are used to convert impedance levels between the input/output ports and the internal impedance used within the filter core. This section will necessarily employ a fair amount of somewhat tedious algebra.

Section III: The third section is devoted to using the preceding results to design 2nd-order tunable bandpass filter.

Section IV: Several real tunable bandpass filters are designed in this section. Fabrication and performance assessment information concludes this section and the paper.

A table of contents is provided on the next page for easier navigation.

1	Introduction	2
1.1	Some History.....	3
1.2	Outline for the Paper	5
2	Admittance and Impedance Inverter Concepts	7
2.1	Lumped-Element Inverters.....	9
3	Filter Core Design Using Admittance Inverters	11
3.1	Filter 3 dB Bandwidth and Filter Core Design.....	12
4	Filter Core Design Using Impedance Inverters.....	16
4.1	Filter 3 dB Bandwidth and Filter Core Design.....	16
5	Input and Output Capacitive-Tapping for Impedance Scaling Purposes.....	19
5.1	Capacitive Tap for Impedance Step-Up	19
5.1.1	An Approximate Solution for C_1 and C_2 in Figure 19	20
5.1.2	Exact Solution for C_1 and C_2 in Figure 19	22
5.1.3	Making the Filter Center Frequency Tunable.....	23
5.2	Capacitive Tap for Impedance Step-Down	24
5.3	Approximate Design Formula for C_1 and C_2	25
5.3.1	Exact Design Formula for C_1 and C_2	26
6	Tunable Bandpass Filter Design Examples.....	28
6.1	Design Formula Summary	28
6.1.1	Topology A in Table 3	29
6.1.2	Topology B in Table 3	30
6.1.3	Topology C in Table 3	30
6.1.4	Topology D in Table 3.....	31
6.2	Design Examples	32
6.2.1	Example 1: 10 MHz to 20 MHz	32
6.2.2	Example 2: 20 MHz to 40 MHz	36
6.2.3	Example 2: 40 MHz to 80 MHz	37
6.2.4	Example 3: 80 MHz to 160 MHz	39
6.2.5	Example 4: 160 MHz to 320 MHz	40
6.2.6	Example 5: 320 MHz to 640 MHz	41
6.3	Example 6: 640 MHz to 1280 MHz	43
6.4	Measured Performance Preliminaries.....	45
6.5	Performance Results.....	45
7	References.....	46
8	Appendix: Inductor Pi-to-Tee Transformation.....	47
9	Appendix: N=2 Tunable Bandpass Filter Design Aid.....	48

2 Admittance and Impedance Inverter Concepts

Even though the bandpass filter order is limited to only two in this paper, it is both computationally helpful as well as insightful to look at the inverter concepts first put forth by Cohn [3, 4, 5, 6, 7, 8] for bandpass filter design. The inverter concepts are particularly helpful in microwave engineering where they are usually implemented as quarter-wavelength segments of transmission line (e.g., microstrip, stripline). As such, filter books without a bent toward microwave engineering will frequently not cover the topic. In this paper, only lumped-element (i.e., LC) inverters will be used as developed herein.

If presented with an impedance/admittance ladder network like the one shown in Figure 6, the input impedance can be written down by inspection as

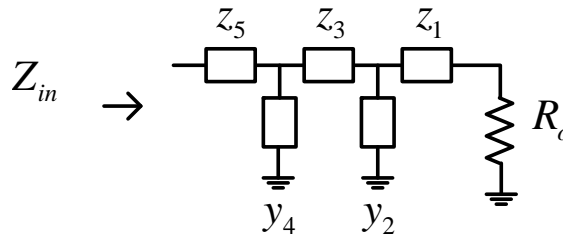


Figure 6 Example ladder network of impedances

$$Z_{in} = z_5 + \frac{1}{y_4 + \frac{1}{z_3 + \frac{1}{y_2 + \frac{1}{z_1 + R_o}}}} \tag{1}$$

in which branch impedance values (at a specified frequency) are denoted by the z_k values and branch admittances are denoted by the y_k values. In this continued-fraction form, impedance (and admittance) inversion steps are clearly visible. If this ladder actually represents a bandpass filter of some kind, it would be natural to think of the z_k branches as series LC sections and the y_k branches as parallel LC sections. In the more general sense, the z_k and y_k branches can also represent individual inductors or capacitors as well.

Going one step further, now consider the cascade shown in Figure 7 where each u_j similarly represents a lossless reactance branch posed by either a LC section, a series capacitor, or a series inductor.

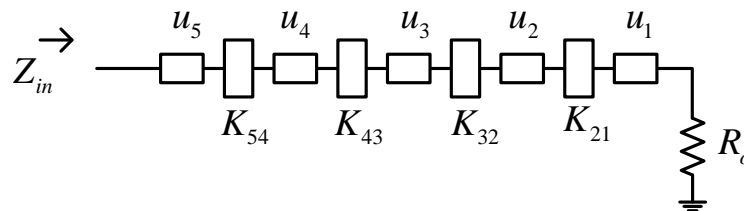


Figure 7 Cascade circuit arrangement using impedance inverters ($K_{i,j}$)

For the moment, also assume that each K -block used in Figure 8 is an ideal impedance inverter which is frequency-independent and governed by the equation

$$K^2 = Z_i Z_o \quad (2)$$

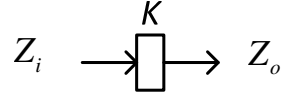


Figure 8 Ideal impedance inverter

Using (2) in connection with Figure 7, the input impedance for the entire cascade can be written as

$$Z_{in} = u_5 + \frac{K_{54}^2}{u_4 + \frac{K_{43}^2}{u_3 + \frac{K_{32}^2}{u_2 + \frac{K_{21}^2}{u_1 + R_o}}} \quad (3)$$

The regularity of this equation along with its similarity to (1) should be self-apparent. This equation can be reorganized as

$$\begin{aligned} Z_{in} &= u_5 + \frac{1}{\frac{u_4}{K_{54}^2} + \frac{K_{43}^2}{K_{54}^2} \frac{1}{u_3 + \frac{K_{32}^2}{u_2 + \frac{K_{21}^2}{u_1 + R_o}}}} \\ &= u_5 + \frac{1}{\frac{u_4}{K_{54}^2} + \left(\frac{K_{54}^2}{K_{43}^2} \right) u_3 + \left(\frac{K_{54}^2 K_{32}^2}{K_{43}^2} \right) \frac{1}{u_2 + \frac{K_{21}^2}{u_1 + R_o}}} \\ &= u_5 + \frac{1}{\frac{u_4}{K_{54}^2} + \left(\frac{K_{54}^2}{K_{43}^2} \right) u_3 + \frac{1}{\left(\frac{K_{43}^2}{K_{54}^2 K_{32}^2} \right) u_2 + \left(\frac{K_{43}^2 K_{21}^2}{K_{54}^2 K_{32}^2} \right) \frac{1}{u_1 + R_o}}} \end{aligned} \quad (4)$$

Based upon (4), it can be seen that Figure 7 can be made equivalent to Figure 6 by choosing the impedance branches u_j and the K values in an appropriate manner.

The beauty of the admittance / impedance inverter concept is that it provides a very straight forward way to design bandpass filters based upon lowpass filter prototype filters. More importantly, it makes it easy to design a wide range of filters with the form shown in Figure 9 and Figure 10 which are well suited for circuit implementation at microwave frequencies. The K -blocks also make it easy to scale impedance levels within

the filter up and down to facilitate other real-world factors like reasonable inductor and capacitance values, etc. An expression similar to (2) applies for admittance inverters as

$$J^2 = Y_i Y_o \tag{5}$$

These concepts ultimately make it possible to design bandpass filters with uniform topologies like that shown in Figure 11. In the balance of this paper, however, only 2nd order bandpass filters like those shown in Table 1 will be considered further.

The next two sections develop the inverter concepts in terms of lumped-element L's and C's. These LC-sections will be key elements of the detailed filter design discussion which follows later.

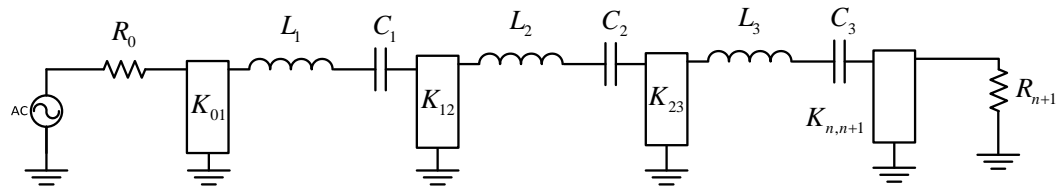


Figure 9 Bandpass filter using impedance inverters

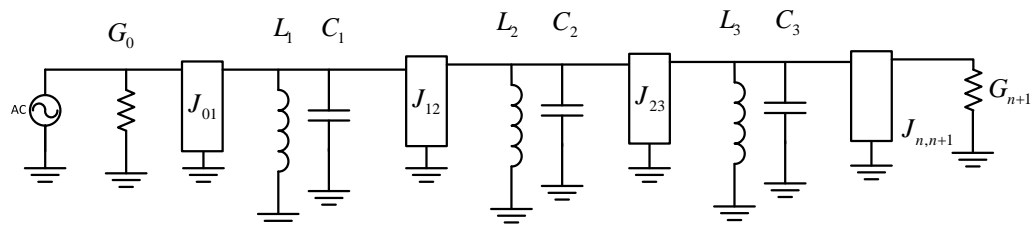


Figure 10 Bandpass filter using admittance inverters

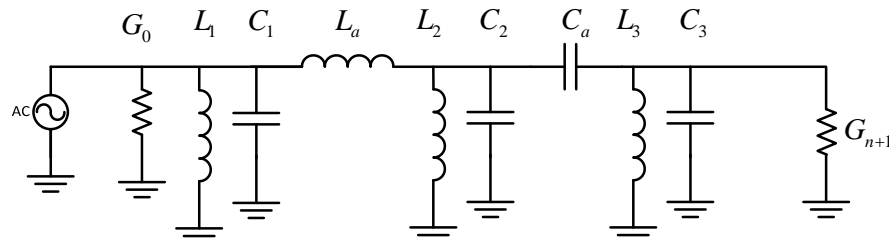


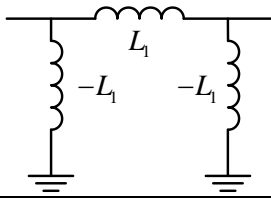
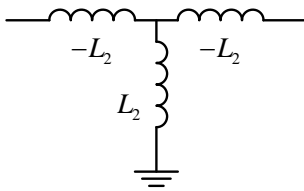
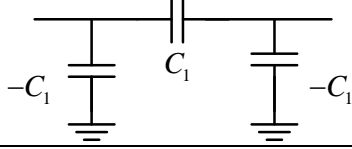
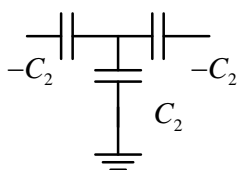
Figure 11 General bandpass filter designs made possible by using inverter concepts

2.1 Lumped-Element Inverters

Approximate lumped-element inverters can be formed in a variety of ways using inductors and capacitors. There is one catch, however. All such inverters require negative L- or C-values which are not physically realizable using passive elements. This problem can usually be sidestepped through later steps in the filter design process though so the negative elements should not pose undue concern at this point in the discussion.

Two admittance inverters and two impedance inverters will be discussed in this section as schematically shown in Table 2. Note that all of the sections entail the use of positive and negative circuit elements as already mentioned and that the positive element is always in the middle position. This generally makes it possible to absorb the negative-valued elements with other positive-valued elements within the filter thereby coming up with a physically realizable filter.

Table 2 Lumped-Element Admittance (a and c) and Impedance (b and d) Inverters

Schematic	Formula	ABCD Matrix
(a) 	$Y_{in}Y_L = J^2$ $J = \frac{1}{\omega_o L_1}$	$\begin{bmatrix} 0 & j\omega_o L_1 \\ \frac{j}{\omega_o L_1} & 0 \end{bmatrix}$
(b) 	$Z_{in}Z_L = K^2$ $K = \omega_o L_2$	$\begin{bmatrix} 0 & -j\omega_o L_2 \\ \frac{-j}{\omega_o L_2} & 0 \end{bmatrix}$
(c) 	$Y_{in}Y_L = J^2$ $J = \omega_o C_1$	$\begin{bmatrix} 0 & \frac{-j}{\omega_o C_1} \\ -j\omega_o C_1 & 0 \end{bmatrix}$
(d) 	$Z_{in}Z_L = K^2$ $K = \frac{1}{\omega_o C_2}$	$\begin{bmatrix} 0 & \frac{j}{\omega_o C_2} \\ j\omega_o C_2 & 0 \end{bmatrix}$

Consider the admittance inverter (a) in Table 2 when its output is terminated into admittance Y_L . The input admittance Y_{in} is given by

$$Y_{in} = \frac{-1}{sL_1} + \left(\frac{1}{\frac{-1}{sL_1} + Y_L} + sL_1 \right)^{-1} \quad (6)$$

$$= \frac{-1}{s^2 L_1^2 Y_L} = \frac{1}{\omega_o^2 L_1^2 Y_L}$$

where ω_o is the radian frequency of interest. This result corresponds to (5) at one specific frequency given $J \equiv \frac{1}{\omega_o L_1}$. Using the *ABCD*-matrix formulation from Part I of this paper, it can be shown that the corresponding *ABCD* matrix for this inverter is given by

$$\begin{aligned}
 ABCD_a(\omega) &= \begin{bmatrix} 1 & 0 \\ \frac{j}{\omega L_1} & 1 \end{bmatrix} \begin{bmatrix} 1 & j\omega L_1 \\ 0 & 1 \end{bmatrix} \begin{bmatrix} 1 & 0 \\ \frac{j}{\omega L_1} & 1 \end{bmatrix} \\
 &= \begin{bmatrix} 0 & j\omega L_1 \\ \frac{j}{\omega L_1} & 0 \end{bmatrix}
 \end{aligned} \tag{7}$$

Similar results can be obtained for the other inverters as summarized in Table 2. These results will be used in the next section of the paper to arrive at design formula for 2nd-order bandpass filters.

3 Filter Core Design Using Admittance Inverters

The discussion has progressed to the point where the core of the filter can be designed using the inverter concepts. What is meant by *filter core* is the portion of the filter less the input and output impedance-scaling networks (e.g., capacitor taps in Figure 1).

A basic 2nd-order bandpass filter is shown in Figure 12. Assuming that the admittance inverter value J_{12} is constant (evaluated at the center frequency of the filter), the input impedance is given by

$$\begin{aligned}
 Z_{in} &= \frac{1 + R_L Y_2}{Y_1 + R_L Y_1 Y_2 + R_L J_{12}^2} \\
 &= \frac{1 + R_L Y}{Y + R_L Y^2 + R_L J_{12}^2} \text{ when } Y_1 = Y_2 = Y
 \end{aligned} \tag{8}$$

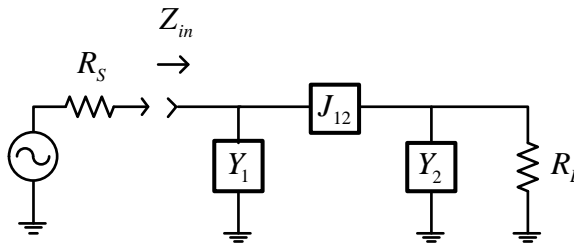


Figure 12 Basic 2nd-order bandpass filter based upon an admittance inverter

Assuming an equally-terminated filter with $R_s = R_L$, the associated input reflection coefficient is given by

$$\begin{aligned}
 \rho &= \frac{Z_{in} - R_s}{Z_{in} + R_s} \\
 &= \frac{1 + R_s Y - R_s (Y + R_s Y^2 + R_s J_{12}^2)}{1 + R_s Y + R_s (Y + R_s Y^2 + R_s J_{12}^2)} \\
 &= \frac{1 - (R_s Y)^2 - (R_s J_{12})^2}{1 + 2R_s Y + (R_s Y)^2 + (R_s J_{12})^2}
 \end{aligned} \tag{9}$$

Based upon (9), the conditions under which $|\rho| = 0$ (assuming J_{12} is constant and independent of frequency) requires

$$1 - (R_S Y)^2 - (R_S J_{12})^2 = 0 \quad (10)$$

For an ideal bandpass filter, Y will be completely imaginary (i.e., a pure reactance) and this point can be amplified by substituting $Y = jY_{re}$. Upon substitution into (10), the result can be simplified to

$$Y_{re} = \pm \sqrt{J_{12}^2 - \frac{1}{R_L^2}} \quad (11)$$

At the filter's center frequency, it is desirable for $Y_{re} = 0$ in order to have minimum insertion loss thereby dictating $J_{12} = \frac{1}{\omega_c L}$ where ω_c is the radian center-frequency of the filter. So long as the two admittance branches exhibit parallel resonance at the filter's center frequency and the condition on J_{12} is met, the filter will exhibit no insertion loss at its center frequency.

3.1 Filter 3 dB Bandwidth and Filter Core Design

The -3 dB points of the filter's frequency response correspond to $|\rho| = \sqrt{2}/2$. From the results just obtained, $R_L J_{12} \equiv 1$. Returning to (9) for the -3 dB frequency points,

$$\frac{\sqrt{2}}{2} = \left| \frac{1 + (R_L Y_{re})^2 - 1}{1 + j2R_L Y_{re} - R_L^2 Y_{re}^2 + 1} \right| \quad (12)$$

leading to $Y_{re} = \pm \sqrt{2}/R_L$ at these points. These results can now be used in the context of the inductively-coupled $N = 2$ bandpass filter shown in Figure 13 to finally arrive at filter-related design formula.

Referring to Figure 13, a simple substitution is made to transform the upper portion of the figure into the lower portion, specifically

$$L_{eff} = L_r \parallel L_c = \frac{L_r L_c}{L_c + L_r} \quad (13)$$

Notice that this re-arrangement now situates a complete admittance inverter between the two LC resonators. Referring now to the lower part of Figure 13 at the -3 dB points

$$Y_{re} = \pm \frac{\sqrt{2}}{R_S} = \omega C_t - \frac{1}{L_{eff} \omega} = \frac{\omega^2 C_t L_{eff} - 1}{\omega L_{eff}} \quad (14)$$

which leads to a quadratic equation in ω given by

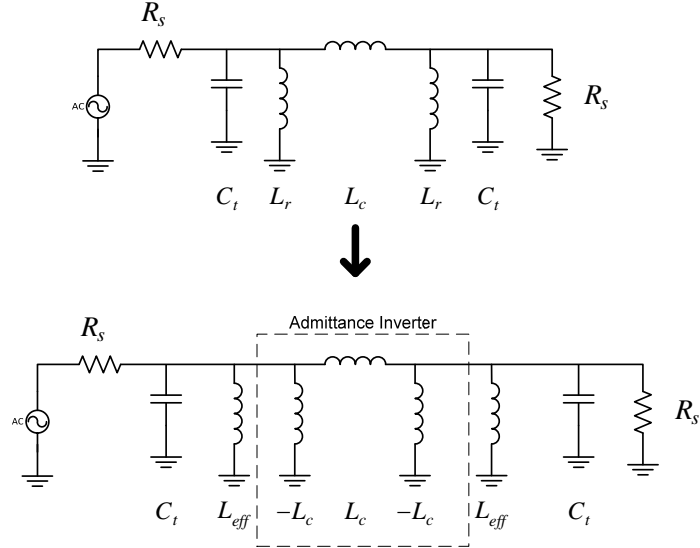


Figure 13 Simplified schematic without input and output tapped capacitors⁴

$$\omega^2 \mp \frac{\sqrt{2}}{R_s} \frac{\omega}{C_t} - \frac{1}{C_t L_{eff}} = 0 \quad (15)$$

The solutions to this quadratic equation are given by

$$\omega_{3dB} = \pm \frac{1}{\sqrt{2}R_s C_t} + \frac{1}{\sqrt{L_{eff} C_t}} \sqrt{1 + \frac{L_{eff}}{2R_s^2 C_t}} \quad (16)$$

From this result, the 3 dB bandwidth is

$$B = \frac{1}{\pi \sqrt{2}R_s C_t} \text{ Hz} \quad (17)$$

and the (arithmetic) center frequency of the filter is given by

$$\omega_c = \frac{1}{\sqrt{L_{eff} C_t}} \sqrt{1 + \frac{L_{eff}}{2R_s^2 C_t}} \quad (18)$$

At a given desired center frequency with a 3 dB filter bandwidth given by (17) and pre-determined core impedance level for the filter (R_s), the one remaining degree of freedom follows from (18) as

$$L_{eff} = \left[\omega_c^2 C_t - \frac{1}{2R_s^2 C_t} \right]^{-1} \quad (19)$$

with

$$C_t = \frac{1}{\pi \sqrt{2}R_s B} \quad (20)$$

⁴ From U22437 Figures for U22436.vsd.

Summarizing, the impedance level R_S is first chosen for the filter. (This will likely be later re-visited to arrive at convenient L and C values.) As established earlier,

$$R_L J_{12} \equiv 1 \text{ and } J_{12} = \frac{1}{\omega_c L_c}. \text{ Therefore,}$$

$$L_c = \frac{R_L}{\omega_c} \quad (21)$$

Based upon the 3 dB filter RF bandwidth B (Hz) chosen for the filter, the required tuning capacitance C_t follows directly from (20). The radian center frequency for the filter ω_c is assumed to be known. The shunt inductance values L_{eff} directly follow from (19). The final shunt inductances L_r in Figure 13 follow from rearranging (13) as

$$L_r = \frac{L_{eff} L_c}{L_c - L_{eff}} \quad (22)$$

A Worked Filter Example

A worked example is always helpful in cementing concepts into place. Assume that a $N = 2$ bandpass filter centered at 250 MHz is desired having a 3 dB bandwidth of 40 MHz. This represents a percentage-bandwidth of 16% which will not unduly press the assumptions behind the admittance inverter concept. Further assume that the impedance level of the filter R_S is chosen to be 200Ω .

From (20), the required tuning capacitance is 28.13 pF. The shunt resonator inductors L_{eff} follow directly from (19) as 14.5 nH. The coupling inductor is given from (21) as 127.3 nH. The value for L_r follows from (22) as 16.36 nH. The corresponding schematic is shown in Figure 14.

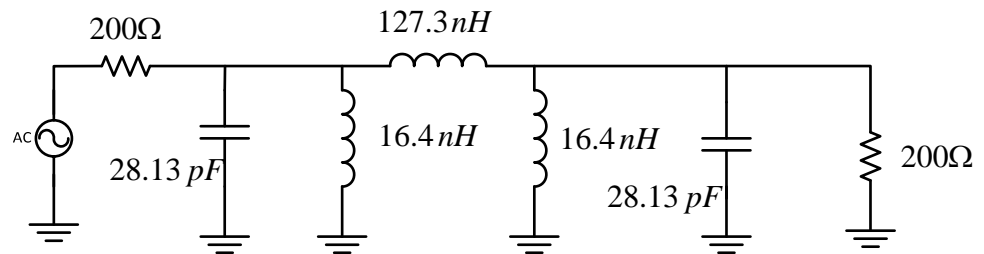


Figure 14 Schematic for example 250 MHz bandpass filter

The frequency response of the filter can be computed using the $ABCD$ matrix methods presented in Part I of this paper. In terms of the top portion of Figure 13, the $ABCD$ matrix for the filter portion (less source and load resistances) is given by

$$ABCD(s) = \begin{bmatrix} 1 & 0 \\ sC_t & 1 \end{bmatrix} \times \begin{bmatrix} 1 & 0 \\ \frac{1}{sL_r} & 1 \end{bmatrix} \times \begin{bmatrix} 1 & sL_c \\ 0 & 1 \end{bmatrix} \times \begin{bmatrix} 1 & 0 \\ \frac{1}{sL_r} & 1 \end{bmatrix} \times \begin{bmatrix} 1 & 0 \\ sC_t & 1 \end{bmatrix} \quad (23)$$

and the S_{11} and S_{21} scattering parameters follow using equations (53) – (55) in Part I of this paper. The resultant frequency response is shown in Figure 15 and Figure 16.

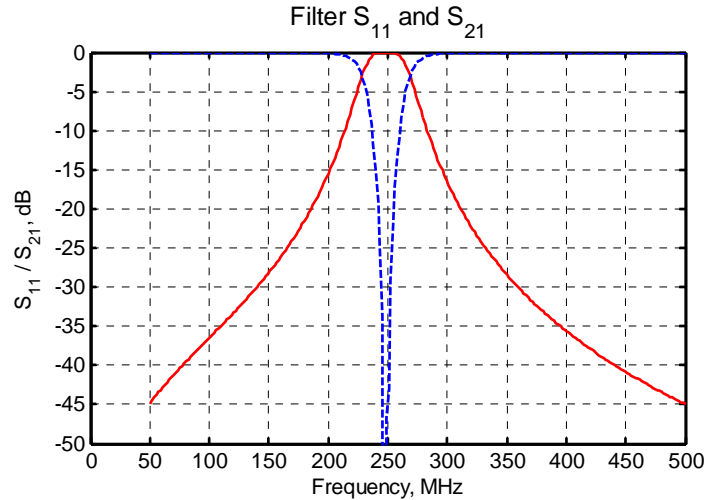


Figure 15 Computed frequency response for the example filter shown in Figure 14

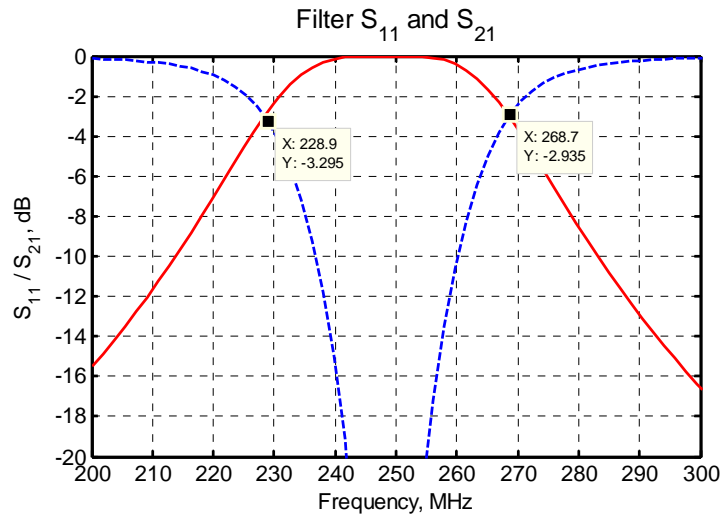


Figure 16 Close-up of frequency response shown in Figure 15

Once the filter is made tunable, it becomes necessary to make the core impedance value R_S a function of the filter's center frequency. Without this provision, the filter's passband will otherwise misbehave badly. The purpose of the tapped-capacitances at the input and output of the filter in Figure 1 can perform this function nicely as developed shortly in §5 of this paper.

4 Filter Core Design Using Impedance Inverters

The inverter discussion would be incomplete if the core filter design topic was not revisited based upon using impedance inverters. The derivation in this section bears substantial similarity to the previous section using admittance inverters.

A 2nd-order bandpass filter using the impedance inverter concept is shown in Figure 17. Taking $Z_1 = Z_2 = Z$, and assuming that the filter's output is terminated with R_S as shown, the input impedance is given by

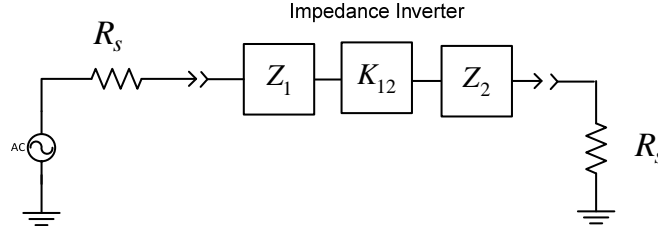


Figure 17 Second-order filter using impedance inverter

$$Z_{in} = \frac{R_S Z + Z^2 + K_{12}^2}{R_S + Z} \quad (24)$$

and the associated input reflection coefficient is given by

$$\rho_{in} = \frac{Z^2 + K_{12}^2 - R_S^2}{Z^2 + K_{12}^2 + 2R_S Z + R_S^2} \quad (25)$$

Assuming that the series impedance branches are both series-resonant at the filter's center frequency in order to present minimum insertion loss, invoking at zero-valued reflection coefficient requires $K_{12} = R_S$ at the resonant frequency thereby leading to

$$K_{12} = \omega_c L_c \quad (26)$$

4.1 Filter 3 dB Bandwidth and Filter Core Design

The -3 dB band-edges of the filter correspond to $|\rho_{in}| = \sqrt{2}/2$. In the context of (25), K_{12} will be assumed to be constant over frequency in order to simplify the analysis. For the filter to be lossless, Z must be a completely imaginary function of frequency which can be denoted by assigning $Z = jZ_{re}$. Using these details in (25) results in

$$\frac{\sqrt{2}}{2} = \left| \frac{-Z_{re}^2 + K_{12}^2 - R_S^2}{-Z_{re}^2 + K_{12}^2 + j2R_S Z_{re} + R_S^2} \right| \quad (27)$$

leading to

$$\frac{1}{2} = \frac{Z_{re}^4}{(2R_S^2 - Z_{re}^2)^2 + 4R_S^2 Z_{re}^2} \quad (28)$$

After a bit more algebra, the solution is $Z_{re} = \pm\sqrt{2}R_S$ at the -3 dB frequency points.

A LC filter which is representative of Figure 17 is shown in the upper portion of Figure 18 with the equivalent physical representation shown in the lower portion.

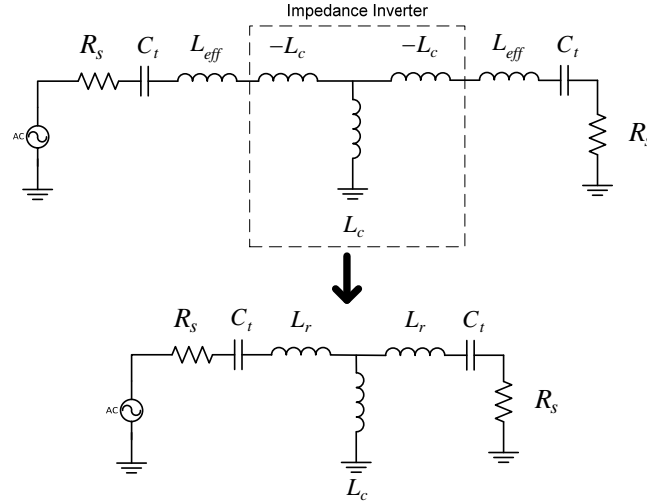


Figure 18 Impedance inverter relationship with physical filter

The simple relationship involved in equating the upper and lower portions of Figure 18 is

$$L_{eff} = L_r + L_c \quad (29)$$

Series resonance was assumed to occur at the center frequency of the filter which is consequently given by

$$\omega_c = \frac{1}{\sqrt{L_{eff}C_t}} \quad (30)$$

Combining this result with (26) produces

$$K_{12} = \omega_c L_c = \frac{L_c}{\sqrt{L_{eff}C_t}} \quad (31)$$

For the Z-branches consisting of L_{eff} in series with C_t at the -3 dB points,

$$Z_{re} = \pm\sqrt{2}R_S = \frac{1}{j} \left(j\omega L_{eff} + \frac{1}{j\omega C_t} \right) \quad (32)$$

leading to a quadratic equation in ω given by

$$\omega^2 L_{eff} C_t \mp \omega C_t \sqrt{2}R_S - 1 = 0 \quad (33)$$

The -3 dB frequency points are finally given by

$$\omega_{3dB} = \frac{1}{\sqrt{L_{eff} C_t}} \sqrt{1 + \frac{R_S^2 C_t}{2L_{eff}}} \mp \frac{R_S}{\sqrt{2L_{eff}}} \quad (34)$$

The arithmetic center frequency for the filter follows as

$$\omega_{arith_center} = \frac{1}{\sqrt{L_{eff} C_t}} \sqrt{1 + \frac{R_S^2 C_t}{2L_{eff}}} \quad (35)$$

and the 3 dB RF bandwidth of the filter is given by

$$B_{-3dBHz} = \frac{R_S}{\sqrt{2\pi L_{eff}}} \text{ Hz} \quad (36)$$

Following through with the remaining details,

$$C_t = \frac{1}{L_{eff} \omega_c^2} \quad (37)$$

$$L_r = L_{eff} - L_c = L_{eff} - \frac{R_S}{\omega_c}$$

Summarizing the design steps, the impedance level for the filter's core R_S , the radian center frequency ω_c , and the filter's 3 dB RF bandwidth are first chosen. The inductance L_{eff} follows directly from (36). Inductor L_c follows from $R_S = \omega_c L_c$, and L_r follows thereafter from (37). The tuning capacitance value C_t is finally given by (30).

The information provided in this section and §3 is sufficient to design 2nd-order bandpass filters using series-LC and parallel-LC resonators at one impedance level given by R_S , but additional measures are needed in order to (i) make the filter designs frequency-tunable and (ii) arrive at convenient LC component values by using impedance scaling between the filter's internal impedance level R_S and the input/output port-impedances which are typically both 50Ω. Both of these measures are accomplished by using capacitive-taps at the input and output of the filters as developed in the next section.

5 Input and Output Capacitive-Tapping for Impedance Scaling Purposes

The tapped-capacitors at the input and output of the filter shown in Figure 1 are used to accomplish several important purposes. First of all, they work together to present each resonator the C_i portion of the resonator shown in Figure 13 and Figure 18. As mentioned at the end of the previous section, the tapped-capacitors make it possible to scale the input and output port impedances (normally 50Ω) up to higher or lower values as needed for constant-Q or constant-bandwidth filters as discussed in §1.1 of Part I of this paper. And finally, the tapped-capacitors add additional transmission zeros to the filter core thereby creating nearly symmetric lower and upper stopband attenuation characteristics. The design formula for tapped-capacitor sections (impedance step-up followed by impedance step-down) are developed in this section.

5.1 Capacitive Tap for Impedance Step-Up

Under appropriate conditions, the tapped capacitors at the input and output ports can be viewed as impedance transformers. In order to see this, consider the input admittance Y of the tapped-capacitor arrangement shown in Figure 19. This admittance is given by

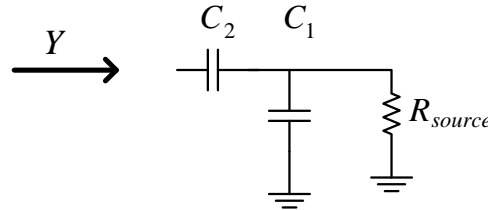


Figure 19 Tapped capacitor configuration for impedance step-up

$$Y = \frac{(j\omega C_2 - \omega^2 R_{source} C_1 C_2) [1 - j\omega R_{source} (C_1 + C_2)]}{1 + \omega^2 R_{source}^2 (C_1 + C_2)^2} \quad (38)$$

from which it follows that

$$\text{Re}[Y] = \frac{1}{R_{source}} \frac{(\omega R_{source} C_2)^2}{1 + \omega^2 R_{source}^2 (C_1 + C_2)^2} \quad (39)$$

Similarly,

$$\text{Im}[Y] = \omega C_2 \frac{1 + \omega^2 R_{source}^2 C_1 (C_1 + C_2)}{1 + \omega^2 R_{source}^2 (C_1 + C_2)^2} \quad (40)$$

Thus far, no approximations have been made and these results are exact.

5.1.1 An Approximate Solution for C_1 and C_2 in Figure 19

Starting from (39) and (40), note that if $\omega^2 R_{source}^2 (C_1 + C_2)^2 \gg 1$ that these results can be approximated by

$$\begin{aligned} \text{Re}[Y] &= \frac{1}{R_{source}} \frac{(\omega R_{source} C_2)^2}{1 + \omega^2 R_{source}^2 (C_1 + C_2)^2} \\ &\Rightarrow \frac{1}{R_{source}} \left(\frac{C_2}{C_1 + C_2} \right)^2 \end{aligned} \quad (41)$$

$$\begin{aligned} \text{Im}[Y] &= \omega C_2 \frac{1 + \omega^2 R_{source}^2 C_1 (C_1 + C_2)}{1 + \omega^2 R_{source}^2 (C_1 + C_2)^2} \\ &\Rightarrow \omega \left(\frac{C_1 C_2}{C_1 + C_2} \right) \end{aligned} \quad (42)$$

Defining

$$n = \frac{C_1 + C_2}{C_2} = 1 + \frac{C_1}{C_2} \quad (43)$$

the source impedance R_{source} is stepped up by a factor of n^2 in (41) and C_t takes the form of C_1 and C_2 in parallel from (42). Note that n is strictly ≥ 1 so the port impedance R_{source} is always stepped-up in magnitude.

The filter design process then follows these next guidelines. Assuming that R_s , ω_c , L_c , C_t and L_{eff} have already been calculated using the formulas in §3.1, the only remaining information required are the values for C_1 and C_2 . It is known that

$$J_{12} = \frac{1}{R_s} = \frac{1}{R_{source} n^2} \quad (44)$$

from which it follows

$$n = \sqrt{\frac{R_s}{R_{source}}} \quad (45)$$

and

$$\frac{C_1}{C_2} = n - 1 \quad (46)$$

From (42) and (46), it must also be true that

$$C_t = \frac{C_1 C_2}{C_1 + C_2} = \frac{n-1}{n} C_2 \quad (47)$$

leading to the final results

$$C_2 = \frac{n}{n-1} C_t \quad (48)$$

$$C_1 = n C_t$$

Example

Picking up where the previous example left off in §3.1 and taking the input and output port impedances to be 50Ω , from (45) $n = 2$. Since $C_t = 28.13$ pF, from (48) $C_2 = 56.26$ pF and $C_1 = 56.26$ pF. The resultant schematic is shown in Figure 20.

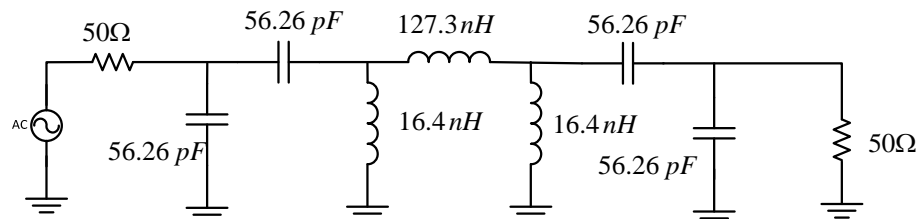


Figure 20 $N = 2$ bandpass filter including tapped-capacitor sections

The $ABCD$ matrix for the reactance-portion of Figure 20 is given by

$$ABCD(s) = \begin{bmatrix} 1 & 0 \\ sC_1 & 1 \end{bmatrix} \times \begin{bmatrix} 1 & \frac{1}{sC_2} \\ 0 & 1 \end{bmatrix} \times \begin{bmatrix} 1 & 0 \\ \frac{1}{sL_r} & 1 \end{bmatrix} \times \begin{bmatrix} 1 & sL_c \\ 0 & 1 \end{bmatrix} \times \begin{bmatrix} 1 & 0 \\ \frac{1}{sL_r} & 1 \end{bmatrix} \times \begin{bmatrix} 1 & \frac{1}{sC_2} \\ 0 & 1 \end{bmatrix} \times \begin{bmatrix} 1 & 0 \\ sC_1 & 1 \end{bmatrix} \quad (49)$$

and the frequency response is shown in Figure 21. Since n is reasonably small, the approximations used in (41) and (42) hold up very well and this response is nearly identical to the first frequency response shown in Figure 15. Notice, however, that the attenuation at 50 MHz is about 5 dB more than in Figure 15 due to the additional transmission zeros from the tapped-capacitor arrangement.

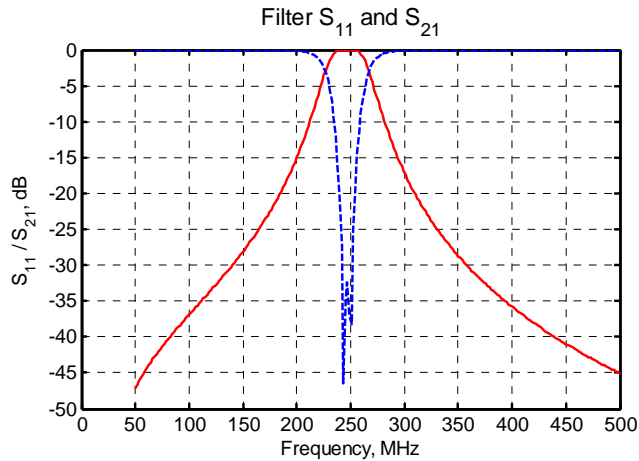


Figure 21 Frequency response of the filter shown in Figure 20 which is very similar to the original filter response shown in Figure 15

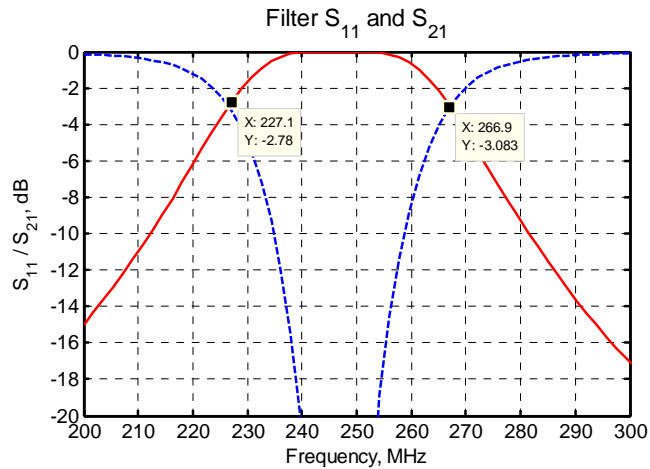


Figure 22 Close-up of the frequency response shown in Figure 21 showing some minor differences compared to Figure 16

5.1.2 Exact Solution for C_1 and C_2 in Figure 19

The preceding section provided an approximate solution for capacitances C_1 and C_2 while shedding some insight into why the tapped-capacitance values behave similarly to a transformer. Exact capacitance solutions are developed in this section.

Consider the equivalent RC networks (at one frequency) shown in Figure 23. The input impedance for the left-hand side of the figure is given by

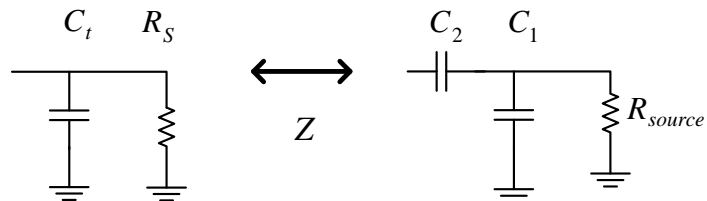


Figure 23 Network equivalence for impedance step-up tapped-capacitor network

$$Z = \left[j\omega C_t + \frac{1}{R_S} \right]^{-1} \quad (50)$$

$$= \frac{R_t (1 - j\omega R_t C_t)}{1 + (\omega R_t C_t)^2}$$

The input impedance for the right-hand portion of the figure is given by

$$Z = \frac{1}{j\omega C_2} + \left(\frac{1 + j\omega R_{source} C_1}{R_{source}} \right)^{-1} \quad (51)$$

$$= \frac{R_{source}}{1 + (\omega R_{source} C_1)^2} - j \left[\frac{\omega R_{source}^2 C_1}{1 + (\omega R_{source} C_1)^2} + \frac{1}{\omega C_2} \right]$$

Equating the real parts of (50) and (51) produces the first key result

$$C_1 = \frac{1}{\omega R_{source}} \sqrt{\left(\frac{R_{source}}{R_t} \right) \left[1 + (\omega R_t C_t)^2 \right]} - 1 \quad (52)$$

Equating the imaginary parts of (50) and (51) produces the second key result

$$C_2 = \left[\frac{\omega^2 R_t^2 C_t}{1 + (\omega R_t C_t)^2} - \frac{\omega^2 R_{source}^2 C_1}{1 + (\omega R_{source} C_1)^2} \right]^{-1} \quad (53)$$

These results are considerably more complicated than the approximate solutions given for C_1 and C_2 in (48) but they are still only exact for the radian frequency ω .

5.1.3 Making the Filter Center Frequency Tunable

A tunable filter requires electronically adjustable capacitor values. As argued earlier in Part I of this paper, it is desirable to leave all of the inductors fixed within the filter and only adjust the capacitance values. This results in (i) capacitance C_t having to change by a factor of 4x to change the filter's center frequency by 2x, and (ii) the filter's core impedance value R_S necessarily being a function of the filter's center frequency.

For best results, the J_{12} and K_{12} values should be based upon the geometric center frequency for the desired tuning range. Therefore, if the filter's center frequency is to be tunable from f_{low} to f_{high} ,

$$f_{geo} = \sqrt{f_{low} f_{high}} \quad (54)$$

and ω_o in Table 2 should be replaced by $\omega_{geo} = 2\pi f_{geo}$.

In order to deal with the frequency-dependent R_S , Figure 23 must be modified to that shown in Figure 24. In this figure, R_{geo} corresponds to R_S at the geometric center frequency of the filter, and parameter γ is a user-specified constant typically chosen to be between 1.0 and 2.0. A γ value of 1.0 corresponds to a constant-Q tunable bandpass

filter whereas a value of 2.0 corresponds to a constant-bandwidth tunable filter. Other rather arbitrary types of R_S frequency dependence could also be chosen of course, like making the filter constant-bandwidth in the lower-half of the tuning range and changing it to be constant-Q in the upper-half.

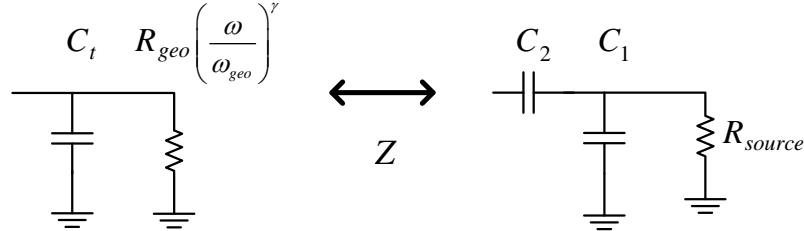


Figure 24 Network equivalence for impedance step-up tapped-capacitor network when center-frequency tunability is to be included

The value for n given earlier in §5.1.1 must be modified as

$$n = \left(\frac{\omega}{\omega_{geo}} \right)^{\gamma/2} \sqrt{\frac{R_{geo}}{R_o}} \tag{55}$$

where $R_{source} = R_{load} = R_o$ has been assumed going forward. The exact design formula given earlier in §5.1.2 must also be modified as

$$C_1 = \frac{1}{\omega R_o} \sqrt{\left(\frac{\omega_{geo}}{\omega} \right)^\gamma \left(\frac{R_o}{R_{geo}} \right) + \omega^2 C_t^2 R_o R_{geo} \left(\frac{\omega}{\omega_{geo}} \right)^\gamma} - 1 \tag{56}$$

$$C_2 = \left[\frac{\omega^2 C_t}{\left(\frac{\omega_{geo}}{\omega} \right)^{2\gamma} \left(\frac{1}{R_{geo}} \right)^2 + (\omega C_t)^2} - \frac{\omega^2 R_o^2 C_1}{1 + (\omega R_o C_1)^2} \right]^{-1} \tag{57}$$

5.2 Capacitive Tap for Impedance Step-Down

The development of the capacitive tap for stepping down the port impedances to a lower internal filter impedance is similar to what was performed in §5.1. The exact result for C_1 and C_2 is a bit more tedious algebraically, however.

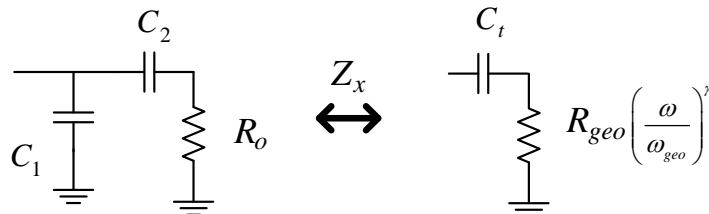


Figure 25 Tapped capacitor configuration for impedance step-down plus its desired equivalent

For the left-hand side of Figure 25, the input impedance is given by

$$Z_x = \frac{1 + j\omega R_o C_2}{-\omega^2 R_o C_1 C_2 + j\omega(C_1 + C_2)} \quad (58)$$

which is to be equated with the input impedance of the right-hand side given by

$$Z_x = R_{geo} \left(\frac{\omega}{\omega_{geo}} \right)^\gamma - \frac{j}{\omega C_t} \quad (59)$$

For simplicity, let

$$R_t = R_{geo} \left(\frac{\omega}{\omega_{geo}} \right)^\gamma \quad (60)$$

Thus far, no approximations have been made.

5.3 Approximate Design Formula for C_1 and C_2

Equating the real parts of (58) and (59) produces

$$R_t = R_o \frac{\left(\frac{C_2}{C_1 + C_2} \right)^2}{1 + (\omega R_o)^2 \left(\frac{C_1 C_2}{C_1 + C_2} \right)^2} \quad (61)$$

If $(\omega R_o)^2 \left(\frac{C_1 C_2}{C_1 + C_2} \right)^2 \ll 1$, equation (61) can be simplified to

$$R_t \cong R_o \left(\frac{C_2}{C_1 + C_2} \right)^2 = \frac{R_o}{n^2} \quad (62)$$

where once again $n \equiv 1 + \frac{C_1}{C_2}$ and the tapped capacitances act similarly to a conventional transformer. Equating the imaginary parts of (58) and (59) produces

$$\frac{1}{\omega C_t} = \frac{\omega^3 R_o^2 C_1 C_2^2 + \omega(C_1 + C_2)}{\omega^4 (R_o C_1 C_2)^2 + \omega^2 (C_1 + C_2)^2} \quad (63)$$

This equation can be rearranged to give

$$C_t = \frac{1 + \left(\omega R_o \frac{C_1 C_2}{C_1 + C_2} \right)^2}{\frac{1}{C_1 + C_2} + (\omega R_o)^2 \frac{C_1 C_2^2}{(C_1 + C_2)^2}} \cong \frac{1}{\frac{1}{C_1 + C_2} + (\omega R_o)^2 \frac{C_1 C_2^2}{(C_1 + C_2)^2}} \quad (64)$$

with the same approximation used in simplifying (61). Multiplying the numerator and denominator by C_t and using the same approximation one more time finally results in

$$C_t \cong C_1 + C_2 \quad (65)$$

Consequently, the approximate solutions are

$$\begin{aligned} C_2 &= \frac{C_t}{n} \\ C_1 &= \left(\frac{n-1}{n} \right) C_t \end{aligned} \quad (66)$$

5.3.1 Exact Design Formula for C_1 and C_2

The exact solution for C_1 and C_2 begins with equating (58) and (59) followed by a cross-multiplication to produce

$$\left(R_t - \frac{j}{\omega C_t} \right) \left[-\omega^2 R_o C_1 C_2 + j\omega (C_1 + C_2) \right] = 1 + j\omega R_o C_2 \quad (67)$$

For the real part,

$$-\omega^2 R_o R_t C_1 C_2 + \frac{C_1 + C_2}{C_t} = 1 \quad (68)$$

For the imaginary portion,

$$\omega R_o \frac{C_1 C_2}{C_t} + \omega R_t (C_1 + C_2) = \omega R_o C_2 \quad (69)$$

which simplifies to

$$\frac{C_1 C_2}{C_t} + \frac{R_t}{R_o} (C_1 + C_2) = C_2 \quad (70)$$

Note that the last two equations are cast in terms of $C_1 C_2$ and $C_1 + C_2$ and therefore not immediately separable. For simplification, let

$$\begin{aligned} a &= -\omega^2 R_o R_t \\ b &= \frac{1}{C_t} \\ d &= \frac{R_t}{R_o} \end{aligned} \quad (71)$$

Equations (68) and (70) can now be rewritten as

$$\begin{aligned} aC_1C_2 + b(C_1 + C_2) &= 1 \\ bC_1C_2 + d(C_1 + C_2) &= C_2 \end{aligned} \quad (72)$$

From the top equation in (72) it follows that

$$C_1C_2 = \frac{1-b(C_1+C_2)}{a} \quad (73)$$

Substituting this result into the lower equation in (72) results in

$$C_2 = \alpha C_1 + \beta \quad (74)$$

with

$$\begin{aligned} \alpha &= \frac{d - \frac{b^2}{a}}{1 + \frac{b^2}{a} - d} \\ \beta &= \frac{\left(\frac{b}{a}\right)}{1 + \frac{b^2}{a} - d} \end{aligned} \quad (75)$$

Substituting (74) back into the top equation in (72) finally produces a quadratic equation in C_1 given by

$$a\alpha C_1^2 + (a\beta + b + b\alpha)C_1 + (b\beta - 1) = 0 \quad (76)$$

The solution to this equation provides C_1 and then C_2 follows directly from using (74).

Returning to R_b , choosing $\gamma = 1$ results in a constant-Q filter whereas choosing $\gamma = 2$ produces a constant-bandwidth filter just as seen earlier in §5.1.3.

6 Tunable Bandpass Filter Design Examples

The primary motivation for these filter topologies is that I intend to build a filter bank for some of my other projects that needs to continuously tune from about 10 MHz through 1400 MHz. Using a switched filter bank (with fixed filters) is hardware prohibitive to say the least. The only plausible way to keep the overall size down is to use a bank of varactor-tuned filters in which each filter covers at least one octave. The bandpass nature of the 2nd order filters makes it possible to have a reasonable filter bank and still suppress 2nd and higher harmonics by 50 dB or more.

When building such a filter bank, inductor values must be kept reasonable due to inductor-Q and self-resonance issues. In addition, using a limited set of common varactor capacitor values will go a long way to help keep the cost down. In this context, the four filter topologies I intend to use are summarized in Table 3.

Table 3 Tunable Filter Topology Candidates

A		$R_o < R_{i\text{internal}}$ Inductor-pi
B		$R_o < R_{i\text{internal}}$ Inductor-tee
C		$R_o > R_{i\text{internal}}$ Inductor-pi
D		$R_o > R_{i\text{internal}}$ Inductor-tee

6.1 Design Formula Summary

The earlier sections of this paper developed a number of perspectives for designing 2nd-order bandpass filters having relatively symmetric lower and upper stopband attenuation characteristics. Admittedly, some design circumstances may actually desire more stopband attenuation in one or the other stopband regions, but only the symmetric stopband case has been considered in this paper.

The four circuit topologies shown in Table 3 are the only topologies being carried forward. There are actually only two different root-topologies (A & C) since the other two topologies can be directly obtained by using a pi-to-tee transformation on the center inductor portion.

Only the exact formula will be used for computing the input and output tapped-capacitance values. The input and output port impedances will be assumed to be equal and represented by R_o .

6.1.1 Topology A in Table 3

The design parameters required to start the design are

f_{low}	Minimum tunable filter center frequency, Hz
f_{high}	Maximum tunable filter center frequency, Hz
B_{geo}	-3 dB RF filter bandwidth, Hz, at the geometric center frequency
R_{geo}	Internal filter impedance at the geometric center frequency of the filter, Ω . Check that R_t given by (60) is always greater than R_o at the band-edges of the filter.
R_o	Port impedance, usually taken to be 50Ω
γ	Constant value per §5.1.3. A value of 1.0 results in a constant-Q filter design whereas a value of 2.0 results in a constant-bandwidth filter design. Any value in between will be a mixture of the two. Inductor-Q values will be more critical as γ is increased.

The geometric center frequency for the filter is

$$\omega_{geo} = 2\pi\sqrt{f_{low}f_{high}} \text{ rad/sec} \quad (77)$$

The coupling inductor L_c is simply

$$L_c = \frac{R_{geo}}{\omega_{geo}} \quad (78)$$

and the total tuning capacitance at the geometric center frequency is given by

$$C_{tgeo} = \frac{1}{\pi\sqrt{2}R_{geo}B_{geo}} \quad (79)$$

Continuing,

$$L_{eff} = \frac{1}{\omega_{geo}^2 C_{tgeo}} \quad (80)$$

and

$$L_r = \frac{L_{eff}L_c}{L_c - L_{eff}} \quad (81)$$

Since the inductance values are fixed in the filter, the total tuning capacitance is given by

$$C_t(\omega) = \left(\frac{\omega_{geo}}{\omega}\right)^2 C_{tgeo} \quad (82)$$

The tuning capacitances C_1 and C_2 are given by

$$C_1 = \frac{1}{\omega R_o} \sqrt{\left(\frac{\omega_{geo}}{\omega}\right)^\gamma \left(\frac{R_o}{R_{geo}}\right) + \omega^2 C_t^2 R_o R_{geo} \left(\frac{\omega}{\omega_{geo}}\right)^\gamma} - 1 \quad (83)$$

$$C_2 = \left[\frac{\omega^2 C_t}{\left(\frac{\omega_{geo}}{\omega}\right)^{2\gamma} \left(\frac{1}{R_{geo}}\right)^2 + (\omega C_t)^2} - \frac{\omega^2 R_o^2 C_1}{1 + (\omega R_o C_1)^2} \right]^{-1} \quad (84)$$

6.1.2 Topology B in Table 3

For this topology, perform all of the computations in the previous section for Topology A, and then convert the inductive-pi (composed of L_r , L_c , and L_r) to a tee-section using the identity in §8.

6.1.3 Topology D in Table 3

The design parameters required to start the design are the same as those specified in §6.1.1 and will not be repeated here.

The geometric center frequency for the filter is

$$\omega_{geo} = 2\pi \sqrt{f_{low} f_{high}} \text{ rad/sec} \quad (85)$$

The coupling inductor L_c is simply

$$L_c = \frac{R_{geo}}{\omega_{geo}} \quad (86)$$

and

$$L_{eff} = \frac{R_{geo}}{\pi \sqrt{2} B_{geo}} \quad (87)$$

From (86) and (87),

$$L_r = L_{eff} - L_c \quad (88)$$

Continuing,

$$C_{tgeo} = \frac{1}{L_{eff} \omega_{geo}^2} \quad (89)$$

and

$$C_t = \left(\frac{\omega_{geo}}{\omega}\right)^2 C_{tgeo} \quad (90)$$

Next, define

$$\begin{aligned}
 R_t &= \left(\frac{\omega}{\omega_{geo}} \right)^\gamma R_{geo} \\
 a &= -\omega^2 R_o R_t \\
 b &= \frac{1}{C_t} \\
 d &= \frac{R_t}{R_o}
 \end{aligned} \tag{91}$$

and compute

$$\begin{aligned}
 \alpha &= \frac{d - \frac{b^2}{a}}{1 + \frac{b^2}{a} - d} \\
 \beta &= \frac{\left(\frac{b}{a} \right)}{1 + \frac{b^2}{a} - d}
 \end{aligned} \tag{92}$$

The solution for C_1 is found by solving the quadratic equation

$$a\alpha C_1^2 + (a\beta + b + b\alpha)C_1 + (b\beta - 1) = 0 \tag{93}$$

and C_2 follows as

$$C_2 = \alpha C_1 + \beta \tag{94}$$

6.1.4 Topology C in Table 3

For this topology, perform all of the computations in the previous section for Topology D, and then convert the inductive-tee (composed of L_r , L_c , and L_l) to a pi-section using the identity in §8.

6.2 Design Examples

Several filter examples will be considered in the following sections. Each frequency range presents its own variety of additional considerations as it pertains to component selection, stray capacitance and stray inductance, and the need for walls around the filter for improved stopband performance. These additional topics are, however, beyond the scope of this paper.

In order to have octave frequency coverage, the maximum-to-minimum capacitance ratio of the varactors must be greater than 4.0. It is also desirable to limit the number of different varactor types involved as well. The chosen varactors are summarized in Table 4.

It is generally insufficient to have the varactors only cover the required capacitance range as this might entail using the varactor with very low reverse-bias voltage values; even zero. This will lead to harmonic distortion and in the extreme case, unexpected distortion resulting from the varactor diodes being over-driven. An example distortion case is shown for the first example in Figure 30 through Figure 34.

Table 4 Varactor Diodes

Part No.	Supplier	Type	Single-Diode Cap(pF) / V	C-Ratio	Q @ 100 MHz, 3V
SMV1253-004LF	Digikey / Skyworks	Common-Cathode SOT-23	37(1) / 4.6(4.7)	12.3	146
SMV1234-004LF	Digikey / Skyworks	Common-Cathode SOT-23	6.5(1) / 2.8(6)	2.8 – 3.4	1800
SMV2022-004LF	Mouser / Skyworks	Common-Cathode SOT-23	7.5(0) / 0.8(15)	6	
SMV1213-004LF	Digikey / Skyworks	Common-Cathode SOT-23	22.8(0.5) / 1.9(8.0)	12	

6.2.1 Example 1: 10 MHz to 20 MHz

----- Design Parameters -----	Inductance Tee: Lr (nH) = 2025.71171 Lc (nH) = 225.07908
>>> Low frequency tuning limit 10.000000, MHz	Inductance Pi: Lr(nH) = 2475.86987 Lc(nH) = 22282.82882
>>> High frequency tuning limit 20.000000, MHz	
>>> Geometric center frequency 14.142136, MHz	
>>> Internal filter impedance at geometric center frequency 20.000000	
>>> Bandwidth at geometric center frequency 2.000000, MHz	Freq, MHz C1, pF C2, pF
>>> gamma 1.000000	-----
	10.00 52.92 60.63
	14.14 20.74 35.86
	20.00 6.99 21.24

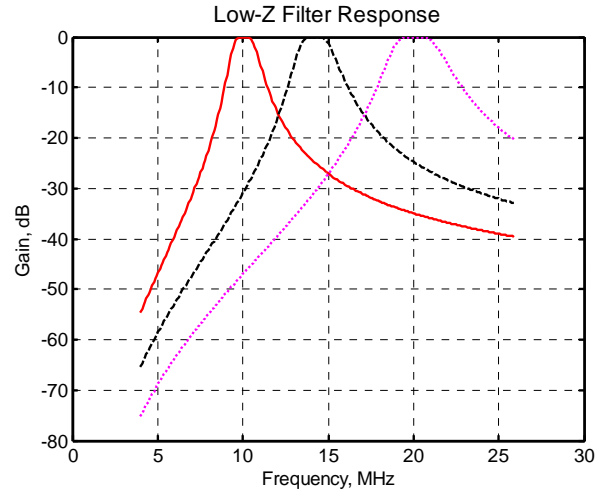


Figure 26 Frequency sweep with ideal LC components

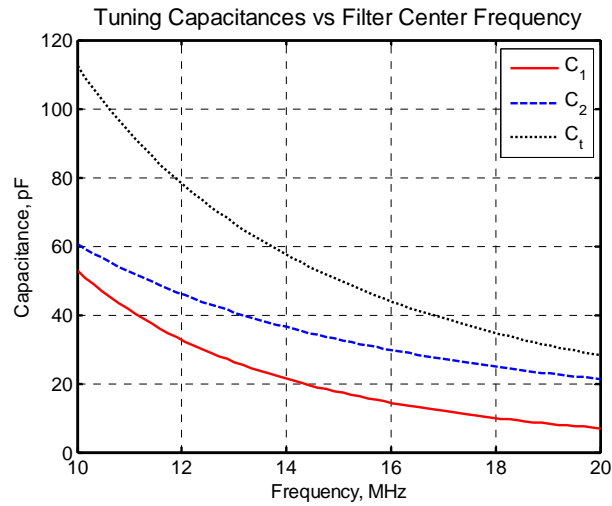


Figure 27 Tuning capacitance values for C_1 and C_2 associated with Figure 26

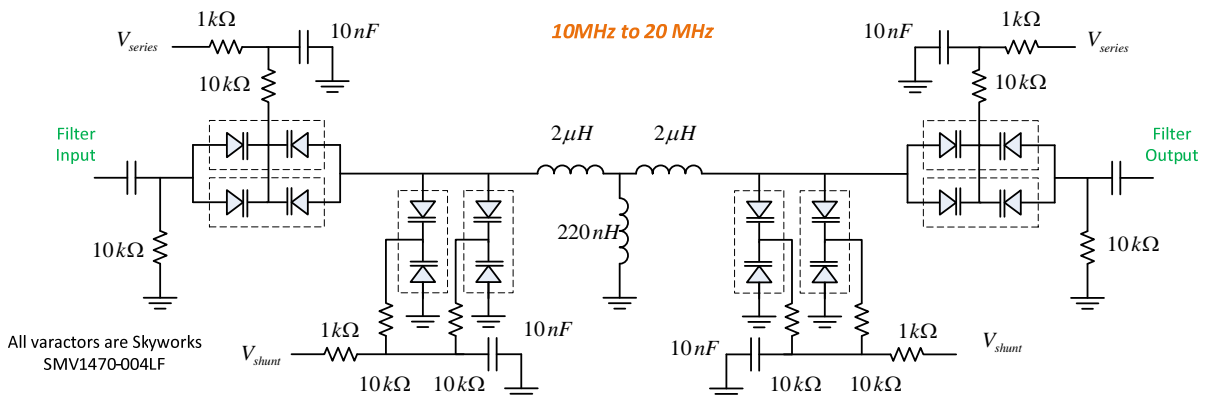


Figure 28 Schematic for 10 MHz to 20 MHz tunable bandpass filter

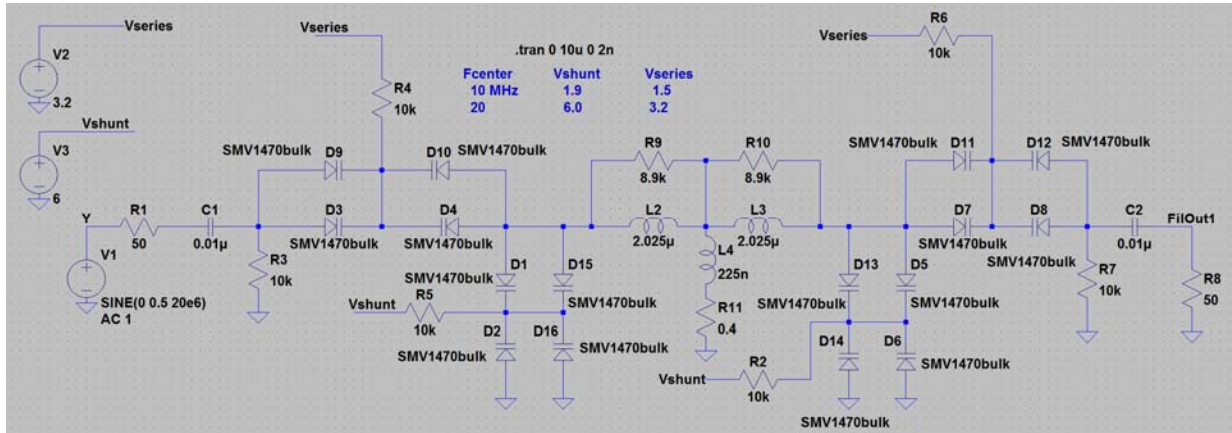


Figure 29 LTspice⁵ schematic version of Figure 28. Inductor Q's at f_{geo} assumed to be 50.

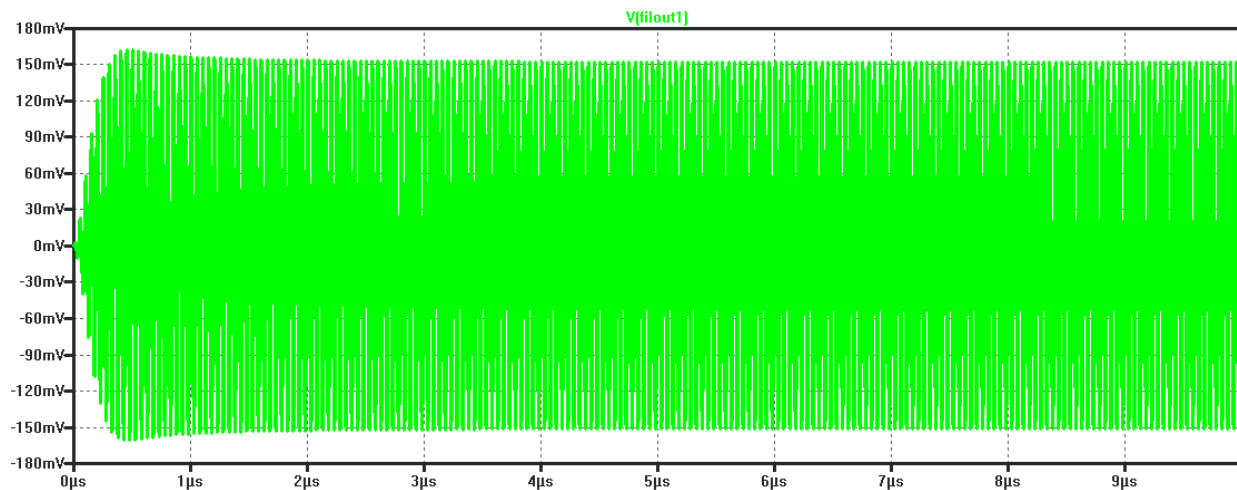


Figure 30 FilOut1 voltage waveform for Figure 29 using input peak-voltage for V1 of 0.5V

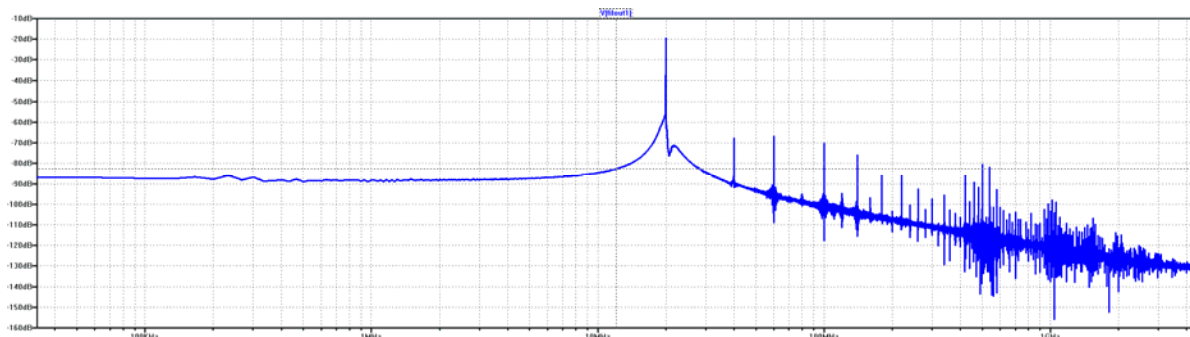


Figure 31 FFT of FilOut1 for V1 magnitude of 0.5V peak. Harmonic distortion terms are visible but other visible distortion elements are likely due to numerical artifacts. Notice that even-order harmonics are substantially suppressed due to using the back-to-back varactors.

⁵ Not all Spice programs are identical. One other Spice program I frequently use limited the model parameter M to 0.90 when in fact it needed to be 39.7 per the SMV1470 datasheet.

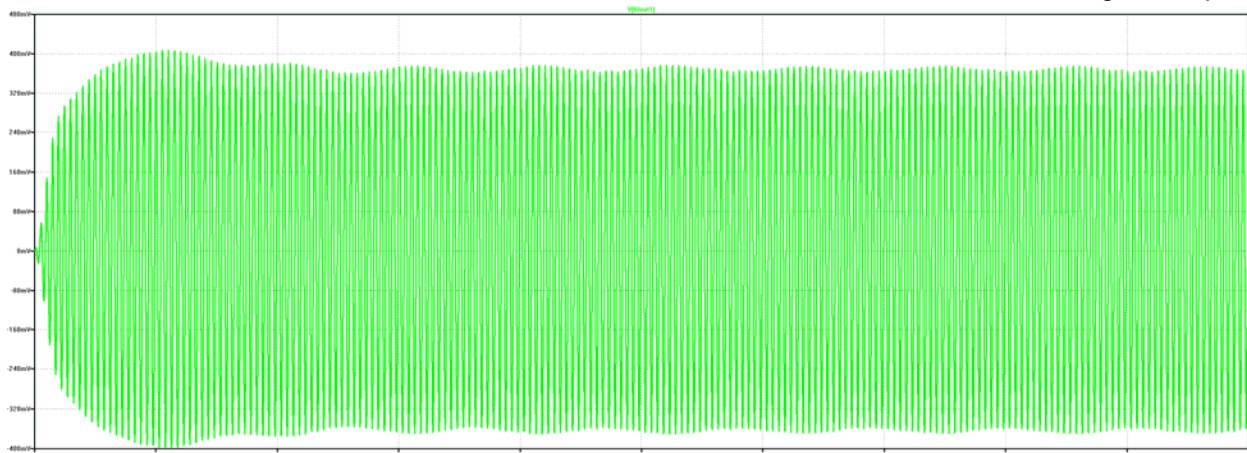


Figure 32 FilOut1 voltage waveform associated with Figure 29 for input peak-voltage for V1 of 1.25V. Nonlinear distortion is becoming visible.

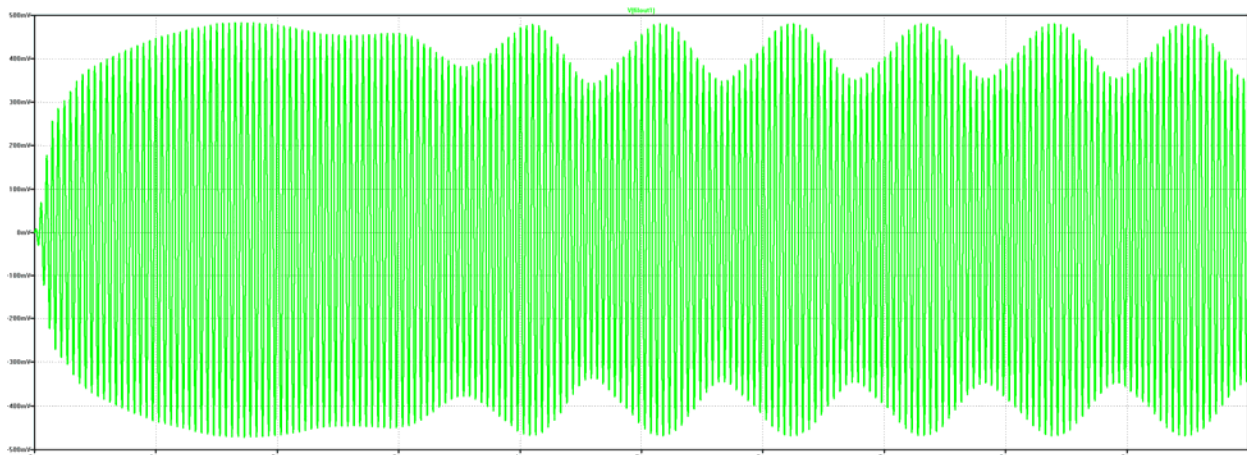


Figure 33 FilOut1 voltage waveform associated with Figure 29 for input peak-voltage for V1 of 1.5V. Nonlinear distortion is now very apparent because varactor(s) are being over-driven

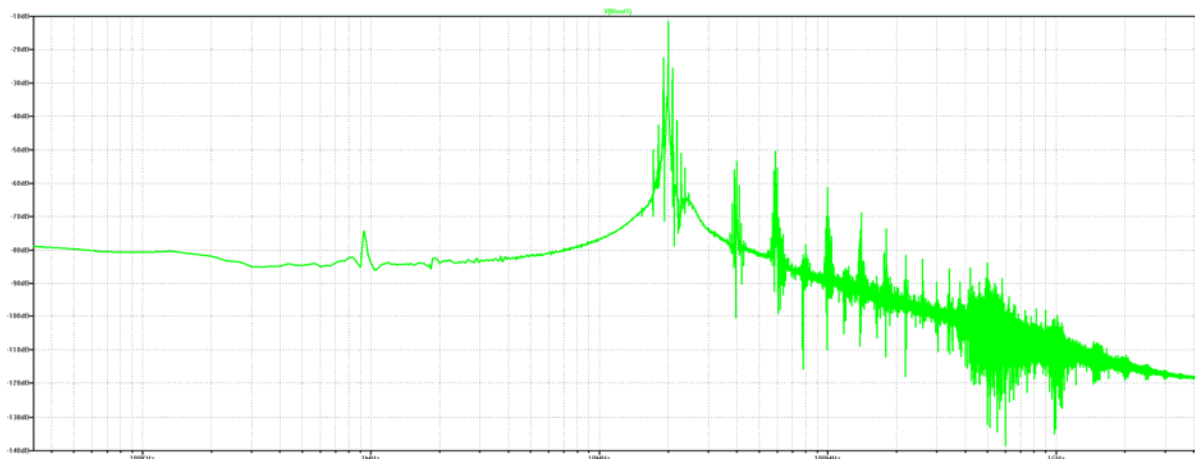


Figure 34 FFT out FilOut1 for V1 magnitude of 1.5V peak. Distortion elements in the spectrum are clearly visible.

6.2.2 Example 2: 20 MHz to 40 MHz

<p>----- Design Parameters -----</p> <p>>>> Low frequency tuning limit 20.000000, MHz >>> High frequency tuning limit 40.000000, MHz >>> Geometric center frequency 28.284271, MHz >>> Internal filter impedance at geometric center frequency 15.000000 >>> Bandwidth at geometric center frequency 3.000000, MHz >>> gamma 1.000000</p>	<p>Inductance Tee: Lr (nH) = 1040.99074 Lc (nH) = 84.40465</p> <p>Inductance Pi: Lr(nH) = 1209.80005 Lc(nH) = 14920.86728</p> <table border="1"> <thead> <tr> <th>Freq, MHz</th> <th>C1, pF</th> <th>C2, pF</th> </tr> </thead> <tbody> <tr> <td>20.00</td> <td>30.45</td> <td>26.19</td> </tr> <tr> <td>28.28</td> <td>12.75</td> <td>15.51</td> </tr> <tr> <td>40.00</td> <td>4.91</td> <td>9.20</td> </tr> </tbody> </table>	Freq, MHz	C1, pF	C2, pF	20.00	30.45	26.19	28.28	12.75	15.51	40.00	4.91	9.20
Freq, MHz	C1, pF	C2, pF											
20.00	30.45	26.19											
28.28	12.75	15.51											
40.00	4.91	9.20											

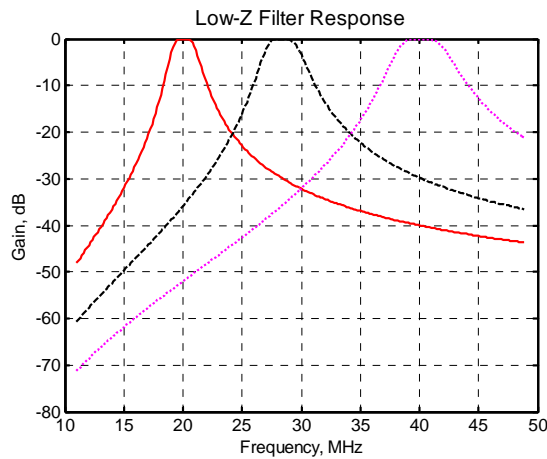


Figure 35 Frequency sweep with ideal LC components

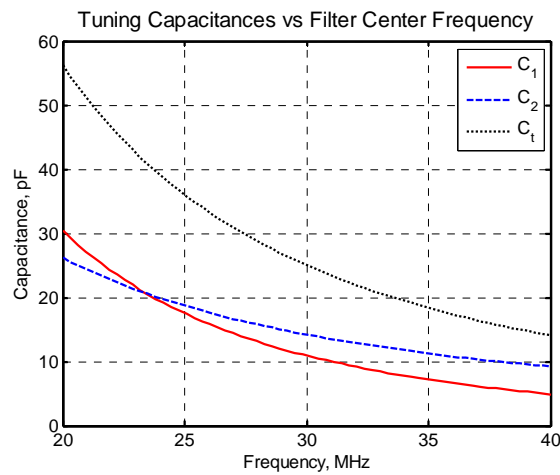


Figure 36 Tuning capacitance values C_1 and C_2 associated with Figure 35

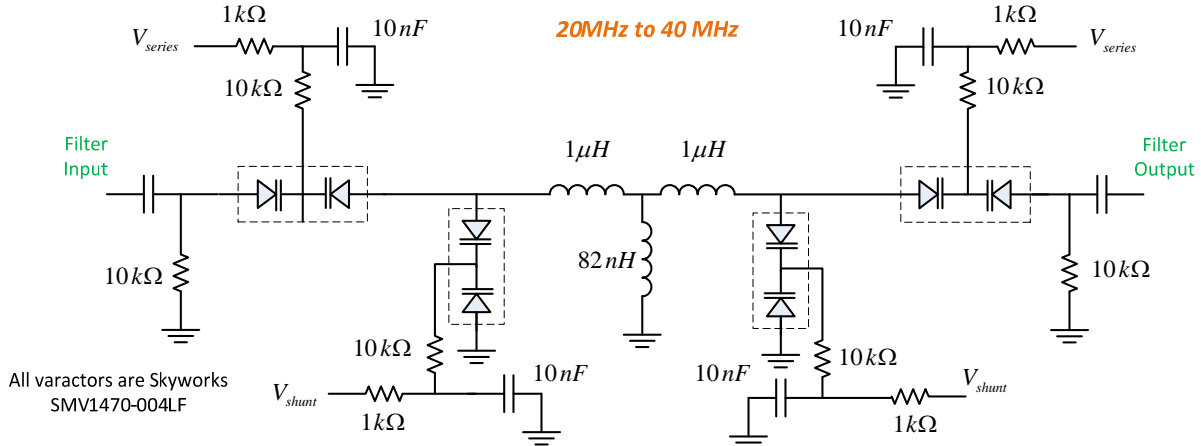


Figure 37 Schematic for 20 MHz to 40 MHz tunable bandpass filter

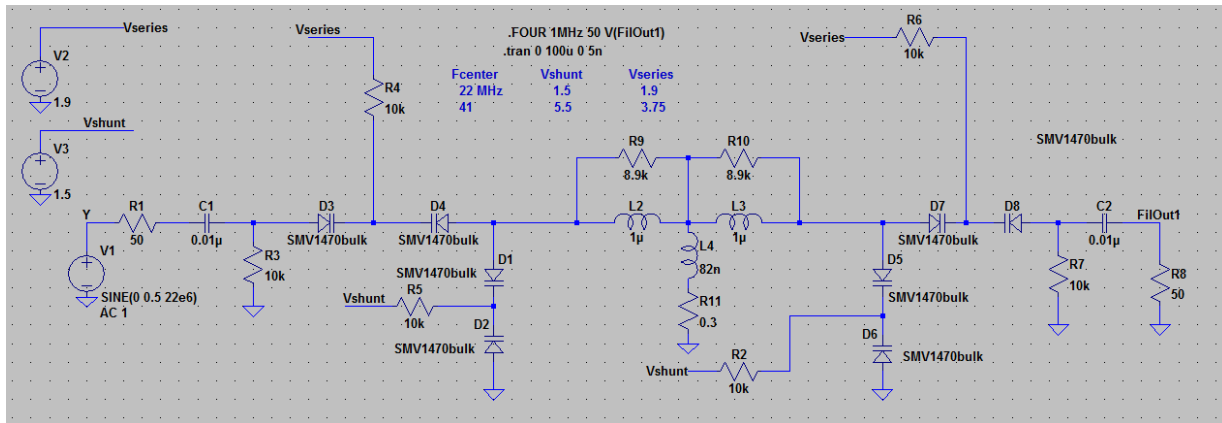


Figure 38 LTSpice schematic version of Figure 37

6.2.3 Example 2: 40 MHz to 80 MHz

Design Parameters		Inductance Tee:	
>>> Low frequency tuning limit 40.000000, MHz		Lr (nH) =	329.64707
>>> High frequency tuning limit 80.000000, MHz		Lc (nH) =	26.72814
>>> Geometric center frequency 56.568542, MHz		Inductance Pi:	
>>> Internal filter impedance at geometric center frequency 9.500000		Lr(nH) =	383.10335
>>> Bandwidth at geometric center frequency 6.000000, MHz		Lc(nH) =	4724.94131
>>> gamma 1.000000		Freq, MHz	C1, pF
			C2, pF
40.00	28.28	16.59	
56.57	12.58	9.80	
80.00	5.36	5.80	

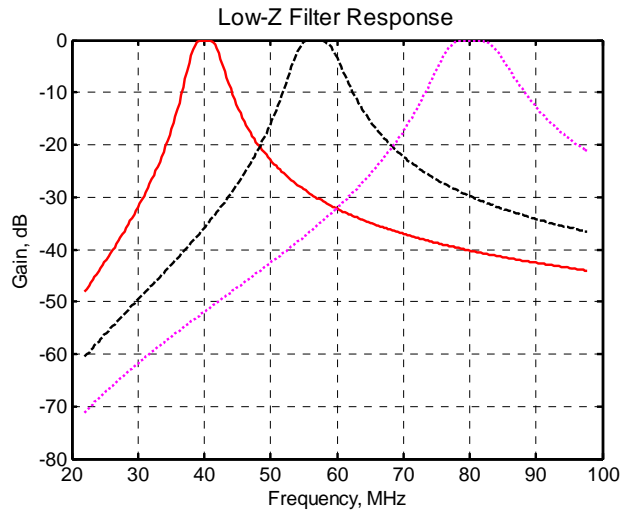


Figure 39 Frequency sweep with ideal LC components

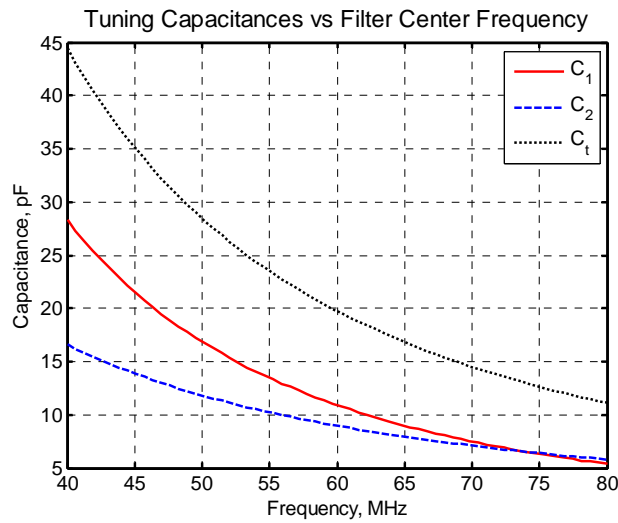


Figure 40 Tuning capacitance values for C_1 and C_2 associated with Figure 39

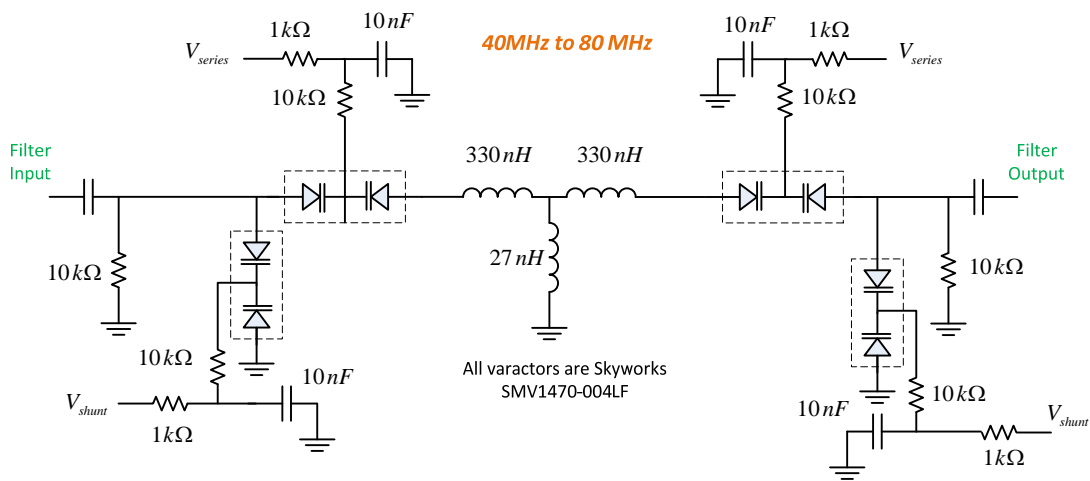


Figure 41 Schematic for 40 MHz to 80 MHz tunable bandpass filter

6.2.4 Example 3: 80 MHz to 160 MHz

Design Parameters		Inductance Tee:		
>>> Low frequency tuning limit 80.000000, MHz		Lr (nH) =	67.99264	
>>> High frequency tuning limit 160.000000, MHz		Lc (nH) =	7.03372	
>>> Geometric center frequency 113.137085, MHz		Inductance Pi:		
>>> Internal filter impedance at geometric center frequency 5.000000		Lr(nH) =	82.06008	
>>> Bandwidth at geometric center frequency 15.000000, MHz		Lc(nH) =	793.24745	
>>> gamma 1.000000		Freq, MHz	C1, pF	C2, pF
		80.00	39.22	14.92
		113.14	18.21	8.69
		160.00	8.29	5.10

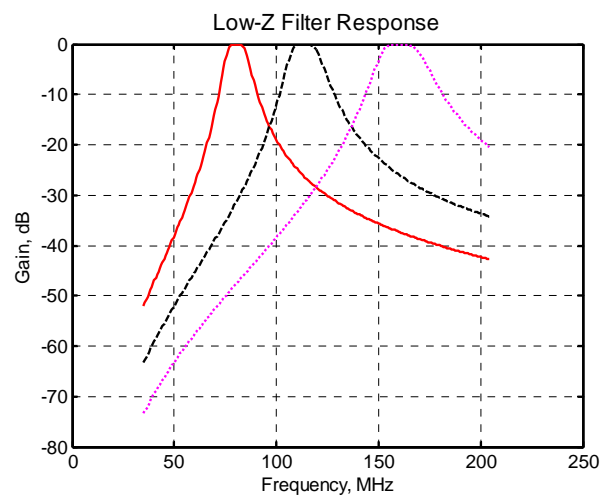


Figure 42 Frequency sweep with ideal LC components

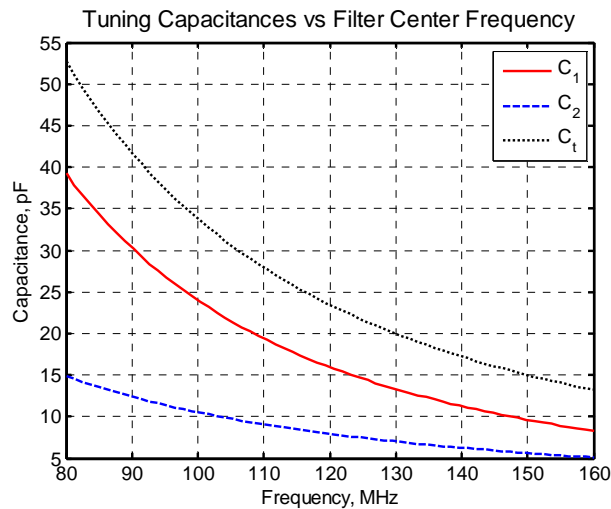


Figure 43 Tuning capacitance values for C₁ and C₂ associated with Figure 42

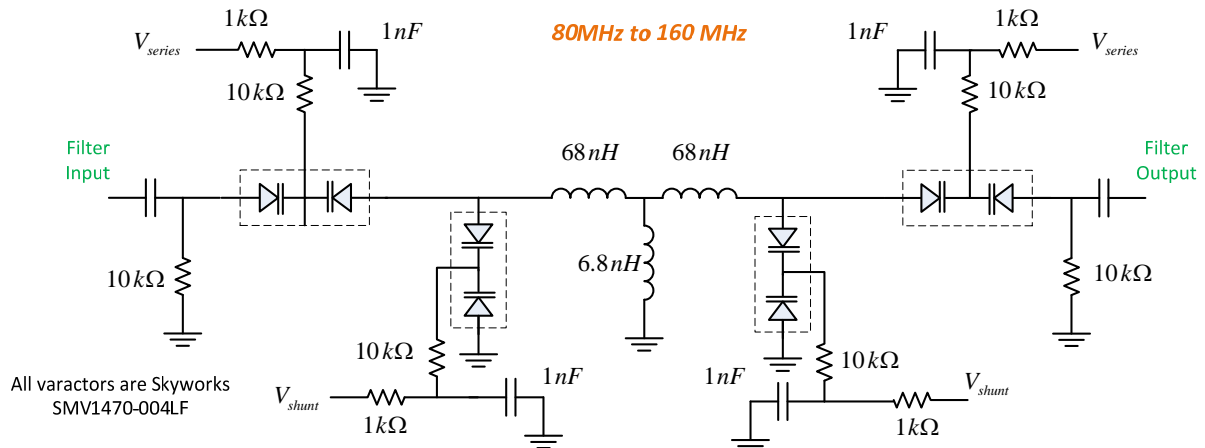


Figure 44 Schematic for 80 MHz to 160 MHz tunable bandpass filter

6.2.5 Example 4: 160 MHz to 320 MHz

Design Parameters		Inductance Pi:		
>>> Low frequency tuning limit 160.000000, MHz		Lr (nH) =	41.72546	
>>> High frequency tuning limit 320.000000, MHz		Lc (nH) =	492.36049	
>>> Geometric center frequency 226.274170, MHz		Inductance Tee:		
>>> Internal filter impedance at geometric center frequency 700.000000		Lr(nH) =	35.67830	
>>> Bandwidth at geometric center frequency 25.000000, MHz		Lc(nH) =	3.02358	
>>> gamma 1.000000		Freq, MHz	C1, pF	C2, pF
		160.00	78.71	37.46
		226.27	46.18	17.40
		320.00	26.92	8.21

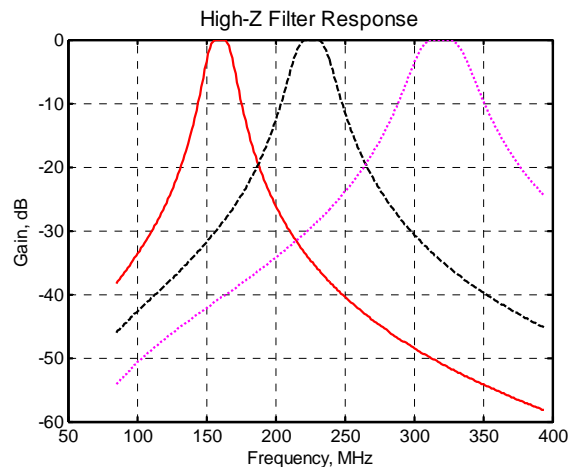


Figure 45 Frequency sweep with ideal LC components

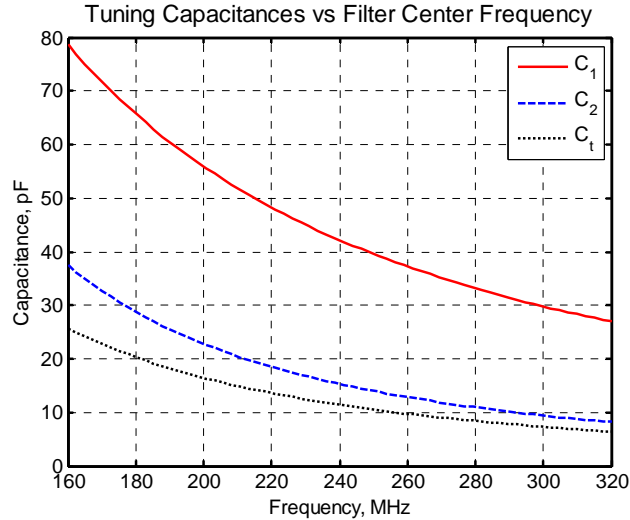


Figure 46 Tuning capacitance values for C_1 and C_2 associated with Figure 45

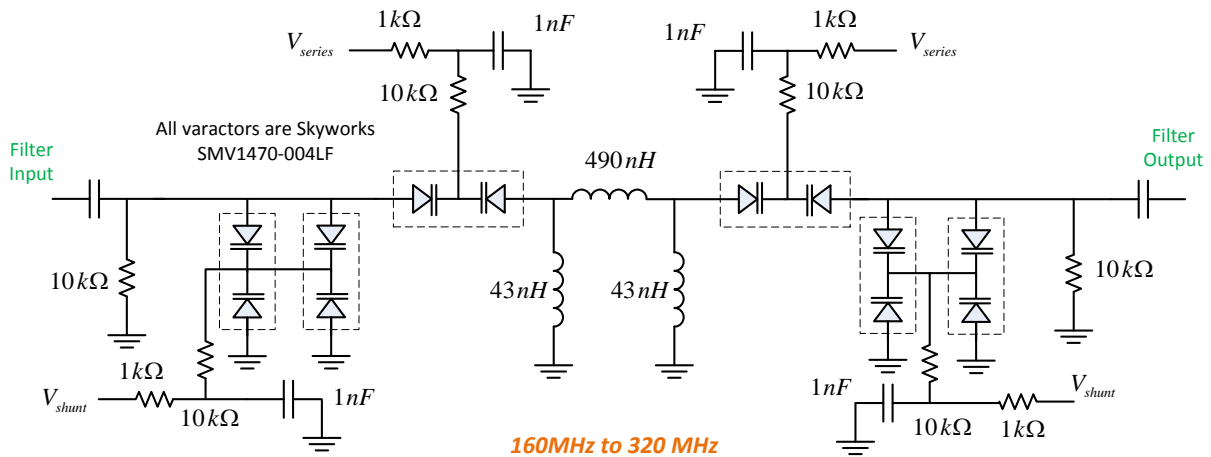


Figure 47 Schematic for 160 MHz to 320 MHz tunable bandpass filter

6.2.6 Example 5: 320 MHz to 640 MHz

Design Parameters		Inductance Pi:		
>>> Low frequency tuning limit 320.000000, MHz >>> High frequency tuning limit 640.000000, MHz >>> Geometric center frequency 452.548340, MHz >>> Internal filter impedance at geometric center frequency 900.000000 >>> Bandwidth at geometric center frequency 50.000000, MHz >>> gamma 1.000000		Lr (nH) =	26.82351	
		Lc (nH) =	316.51745	
		Inductance Tee:		
		Lr(nH) =	22.93605	
		Lc(nH) =	1.94373	
		Freq, MHz	C1, pF	C2, pF
		320.00	34.39	13.79
		452.55	20.09	6.48
		640.00	11.64	3.08

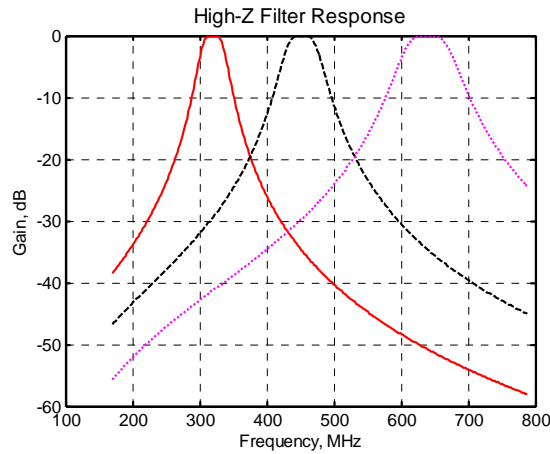


Figure 48 Frequency sweep with ideal LC components

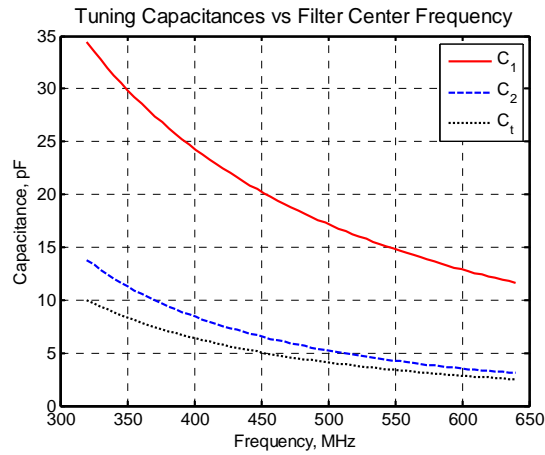


Figure 49 Tuning capacitance values for C_1 and C_2 associated with Figure 48

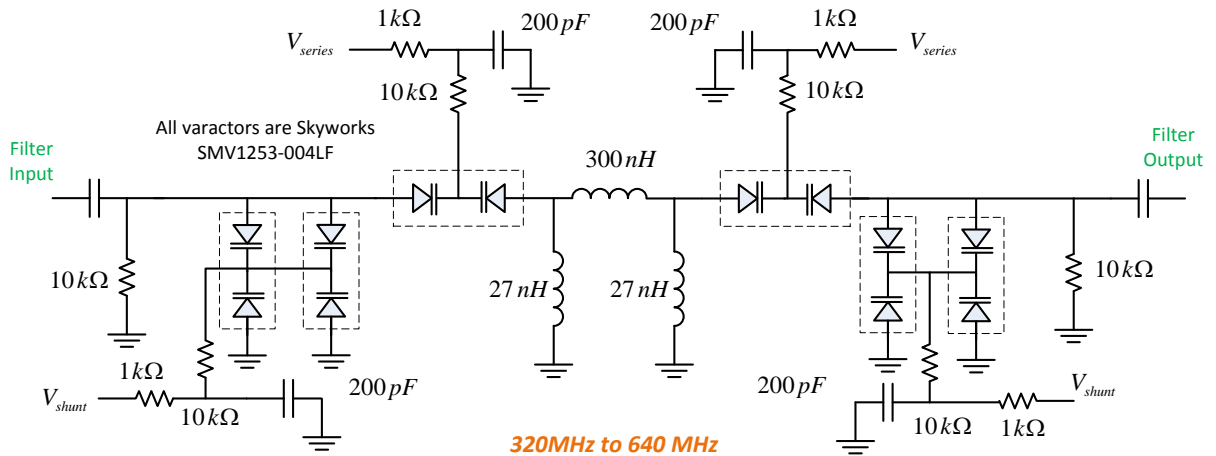


Figure 50 Schematic for 320 MHz to 640 MHz tunable bandpass filter

6.3 Example 6: 640 MHz to 1280 MHz

Design Parameters		Inductance Pi:		
>>> Low frequency tuning limit 640.000000, MHz		Lr (nH) =	7.30196	
>>> High frequency tuning limit 1280.000000, MHz		Lc (nH) =	86.16308	
>>> Geometric center frequency 905.096680, MHz		Inductance Tee:		
>>> Internal filter impedance at geometric center frequency 490.000000		Lr(nH) =	6.24370 ⁶	
>>> Bandwidth at geometric center frequency 100.000000, MHz		Lc(nH) =	0.52913	
>>> gamma 1.000000		Freq, MHz	C1, pF	C2, pF
		-----	-----	-----
		640.00	23.74	14.74
		905.10	13.99	6.71
		1280.00	8.21	3.11

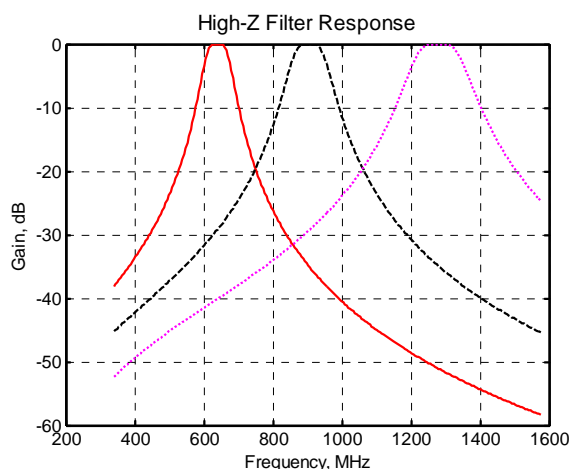


Figure 51 Frequency sweep with ideal LC components

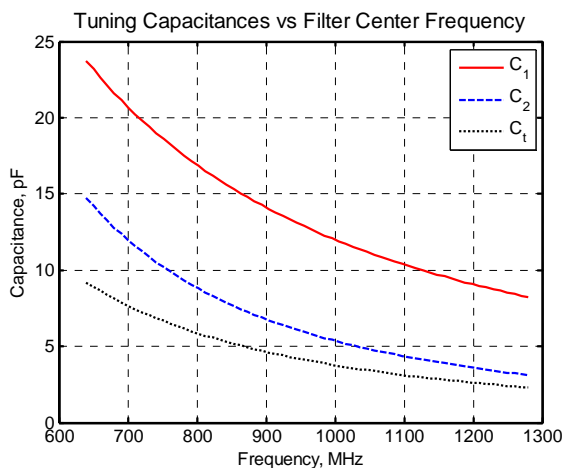


Figure 52 Tuning capacitance values for C₁ and C₂ associated with Figure 51

⁶ 4.9 nH in the schematic Figure 53 to account for stray inductance of varactors.

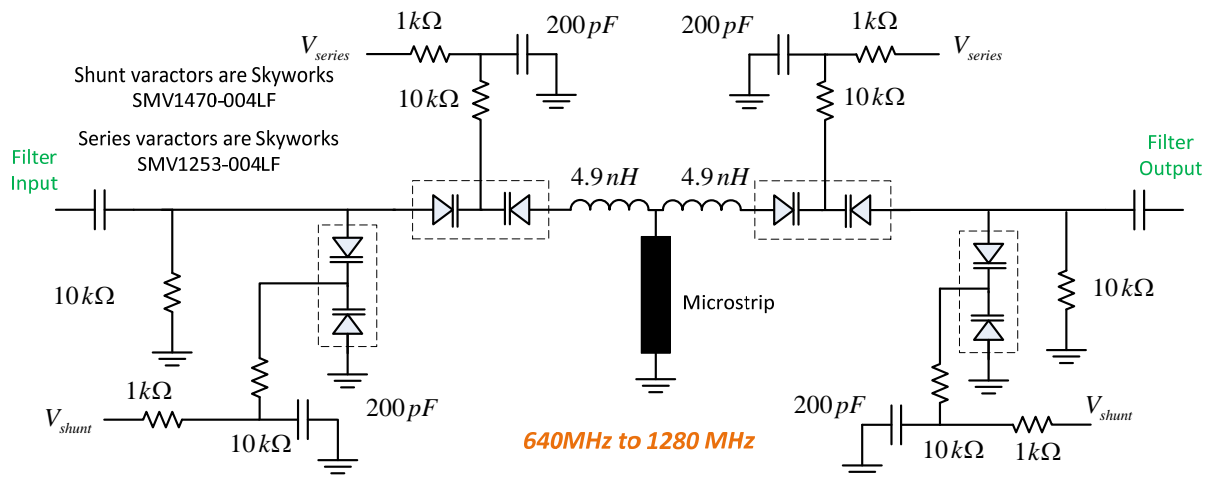


Figure 53 Schematic for 640 MHz to 1280 MHz tunable bandpass filter. Shunt inductive element is microstrip representing about 0.53 nH.

6.4 Measured Performance Preliminaries

A means for tuning each filter is required before any filter characterization can be done. Since the varactor-pairs are not necessarily matched devices, two independent series-tune voltages and two independent parallel-tune voltages are ideally required. Depending upon the results, it may also be desirable to slave the voltages to one another so that only one series and one parallel tune voltage value are used.

Rather than arrange four laboratory voltage supplies to provide these tuning voltages, it proved more convenient to program an Arduino Uno microprocessor to provide the voltages by way of its PWM analog outputs. These outputs must be heavily filtered of course, but this was anticipated early on in the project and posed no additional requirements. A photograph of the circuitry involved is shown in Figure 54. The LCD display was configured with individual *sliders* for individually controlling each tuning voltage and the corresponding voltage is shown numerically in mV to the right of each respective slider. The toggle switches at the bottom make it a simple matter to slave the two series voltages and or two parallel tuning voltages together.

The filtered PWM output voltages are increased by a factor of 3 and further filtering applied on the prototype filter board. The varactor tuning voltages can consequently span from about 0V up to about 15V.



Figure 54 Arduino Uno with attached LCD panel for creation of varactor tuning voltages. Touch-sliders on the panel are used to individually adjust all four tuning voltages while the toggle switches make it possible to also slave the series and or parallel voltages to one another. The numerical display readout is in mV for each respective voltage.

6.5 Performance Results

Owing to the length of this memo, the final performance results will be presented in Part III.

7 References

1. Richard W. Daniels, *Approximation Methods for Electronic Filter Design*, McGraw-Hill Book, 1974.
2. J.A. Crawford, "Advanced Manpack Radio Concept for UHF DAMA Satellite Communications," SBIR AF91-030, March 1992.
3. George L. Matthaei, Leo Young, and E.M.T. Jones, *Microwave Filters, Impedance-Matching Networks, and Coupling Structures*, Artech House, 1980.
4. Gabor C. Temes and Sanjit K. Mitra, *Modern Filter Theory and Design*, John Wiley & Sons, 1973.
5. W. Alan Davis, *Microwave Semiconductor Circuit Design*, Van Nostrand Reinhold, 1984.
6. Gabor C. Temes and Sanjit K. Mitra, *Modern Filter Theory and Design*, John Wiley & Sons, 1973.
7. J. A. G. Malherbe, *Microwave Transmission Line Filters*, Artech House, 1979.
8. Peter A. Rizzi, *Microwave Engineering Passive Circuits*, Prentice-Hall, 1988.

8 Appendix: Inductor Pi-to-Tee Transformation

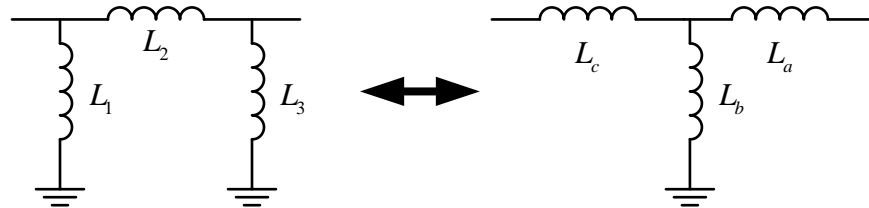


Figure 55 Inductor pi-to-tee equivalences as given by (95) and (96)

$$L_1 = \frac{\Delta_L}{L_a}$$

$$L_2 = \frac{\Delta_L}{L_b}$$

$$L_3 = \frac{\Delta_L}{L_c}$$

$$\Delta_L = L_a L_b + L_b L_c + L_a L_c$$

$$L_a = \frac{L_2 L_3}{\Sigma_L}$$

$$L_b = \frac{L_1 L_3}{\Sigma_L}$$

$$L_c = \frac{L_1 L_2}{\Sigma_L}$$

$$\Sigma_L = L_1 + L_2 + L_3$$
(95)

$$L_a = \frac{L_2 L_3}{\Sigma_L}$$

$$L_b = \frac{L_1 L_3}{\Sigma_L}$$

$$L_c = \frac{L_1 L_2}{\Sigma_L}$$

$$\Sigma_L = L_1 + L_2 + L_3$$
(96)

9 Appendix: N=2 Tunable Bandpass Filter Design Aid

```

%===== u24160_filter_design_aid.m =====
%
% N=2 Tunable Bandpass Filter Design Aid
% u24160 May, 2017
% Copyright 2017 AM1 LLC
%
function u24160_filter_design_aid()
%
global Ro;
global Rgeo;
global gamma;
global flow;
global fhigh;
global Bgeo;
global pi;
global wgeo;
global Ctgeo;

pi= 3.141592654;
Ro= 50;
Rgeo= 200;
gamma= 1;
flow= 10;
fhigh= 25;
Bgeo= 2;

loop= true;
while( loop )
%
%
disp( '1 Enter flow, MHz' );
disp( '2 Enter fhigh, MHz' );
disp( '3 Enter Rgeo' );
disp( '4 Enter bandwidth at fgeo, MHz' );
disp( '5 gamma' );
disp( ' ' );
disp( '6 C O M P U T E' );
disp( ' ' );
disp( '9 Display design parameters' );
disp( '0 Exit' );
disp( ' ' );

vx= input( '??', 's' );

switch( vx )
case '1'
    flow= input( 'Flow, MHz ' );
case '2'
    fhigh= input( 'Fhigh, MHz ' );
case '3'
    Rgeo= input( 'Rgeo ' );
case '4'
    Bgeo= input( 'Bgeo, MHz' );
case '5'
    gamma= input( ' gamma ' );
case '6'

```



```

        compute();
    case '9'
        disp( '-----' );
        disp( '          Design Parameters          ' );
        disp( '-----' );
        disp( num2str( flow, '>>> Low frequency tuning limit %f, MHz'
) );
        disp( num2str( fhigh, '>>> High frequency tuning limit %f,
MHz' ) );
        disp( num2str( sqrt(flow*fhigh), '>>> Geometric center
frequency %f, MHz' ) );
        disp( num2str( Rgeo, '>>> Internal filter impedance at
geometric center frequency %f' ) );
        disp( num2str( Bgeo, '>>> Bandwidth at geometric center
frequency %f, MHz' ) );
        disp( num2str( gamma, '>>> gamma %f' ) );
        disp( ' ' );
    case '0'
        loop= false;
    end
    %wgeo= sqrt( flow*fhigh )*2*pi*1e6;
    %Ctgeo= 1/( sqrt(2)*pi*Rgeo*Bgeo );
end
end
%=====
%
%
function compute()
%
global Ro;
global Rgeo;
global gamma;
global flow;
global fhigh;
global Bgeo;
global pi;
global wgeo;
global Ctgeo;

if( Rgeo > Ro )
    %
    %   Core impedance is > Ro
    %
    fgeo= sqrt(flow*fhigh);
    Ctgeo= 1/(sqrt(2)*pi*Rgeo*Bgeo*1e6);
    wgeo= 2*pi*fgeo*1e6;
    Lc= Rgeo/wgeo;
    Leff= 1/(wgeo^2 * Ctgeo);
    Lr= Leff*Lc/(Lc - Leff);
    %
    %   Look at values at flow, fgeo, and fhigh
    %
    wlow= 2*pi*flow*1e6;
    whigh= 2*pi*fhigh*1e6;
    wgeo= sqrt(wlow*whigh);

    [C1xlow, C2xlow]= C12forHighZ(wlow);
    [C1xgeo, C2xgeo]= C12forHighZ(wgeo);
    [C1xhigh, C2xhigh]= C12forHighZ(whigh);

```

```

disp( 'Inductance Pi:' );
disp( num2str( Lr*1e9, 'Lr (nH) = %15.5f' ) );
disp( num2str( Lc*1e9, 'Lc (nH) = %15.5f' ) );
disp( ' ' );
disp( 'Inductance Tee:' );
[Ltee_a, Ltee_b, Ltee_c]= Lpi2tee( Lr, Lc, Lr );
disp( num2str( Ltee_a*1e9, 'Lr(nH) = %15.5f' ) );
disp( num2str( Ltee_b*1e9, 'Lc(nH) = %15.5f' ) );

disp( ' ' );
disp( 'Freq, MHz      C1, pF      C2, pF      ' );
disp( '-----' );
disp( [num2str( flow, '%8.2f' ), ' ', num2str( C1xlow*1e12, '%8.2f' )
num2str( C1xlow*1e12, '%8.2f' ), ' ', num2str( C2xlow*1e12, '%8.2f' )
] );
disp( [num2str( fgeo, '%8.2f' ), ' ', num2str( C1xgeo*1e12, '%8.2f' )
num2str( C1xgeo*1e12, '%8.2f' ), ' ', num2str( C2xgeo*1e12, '%8.2f' )
] );
disp( [num2str( fhigh, '%8.2f' ), ' ', num2str( C1xhigh*1e12, '%8.2f' )
num2str( C1xhigh*1e12, '%8.2f' ), ' ', num2str( C2xhigh*1e12, '%8.2f' )
] );

fig1= figure(1);
clf;
axes( 'FontName', 'Arial', 'FontSize', 12 );

Npts= 256;
ii=1:Npts;
fswp= flow-3*Bgeo + (fhigh-flow+6*Bgeo)*(ii-1)/Npts;
[gaindB]= sweepHighZnet( fswp, Lr, Lc, C1xlow, C2xlow );
p1= plot( fswp, gaindB, 'r' );
set( p1, 'LineWidth', 2 );
hold on

[gaindB]= sweepHighZnet( fswp, Lr, Lc, C1xgeo, C2xgeo );
p1= plot( fswp, gaindB, 'k--' );
set( p1, 'LineWidth', 2 );
hold on

[gaindB]= sweepHighZnet( fswp, Lr, Lc, C1xhigh, C2xhigh );
p1= plot( fswp, gaindB, 'm:' );
set( p1, 'LineWidth', 2 );
hold on

grid on
xlabel( 'Frequency, MHz', 'FontName', 'Arial', 'FontSize', 12 );
ylabel( 'Gain, dB', 'FontName', 'Arial', 'FontSize', 12 );
title( 'High-Z Filter Response', 'FontName', 'Arial', 'FontSize', 14
);

h= gca;
set( h, 'LineWidth', 2 );

%
% Plot tuning capacitances versus frequency
%
Np= 64;
jk=1:Np;
fswp= ( flow + (fhigh-flow)*(jk-1)/(Np-1) );
fgeo= sqrt(flow*fhigh);

```

```

for jk=1:Np
    [C1y, C2y]= C12forHighZ(2*pi*fswp(jk)*1e6);
    C1p(jk)= C1y*1e12;
    C2p(jk)= C2y*1e12;
    Ctp(jk)= (fgeo/fswp(jk))^2 * Ctgeo * 1e12;
end
figure(2);
clf;
axes( 'FontName', 'Arial', 'FontSize', 12 );
p1= plot( fswp, C1p, 'r' );
set( p1, 'LineWidth', 2 );
hold on
p1= plot( fswp, C2p, 'b--' );
set( p1, 'LineWidth', 2 );
hold on
p1= plot( fswp, Ctp, 'k:' );
set( p1, 'LineWidth', 2 );

grid on
xlabel( 'Frequency, MHz', 'FontName', 'Arial', 'FontSize', 12 );
ylabel( 'Capacitance, pF', 'FontName', 'Arial', 'FontSize', 12 );
title( 'Tuning Capacitances vs Filter Center Frequency', 'FontName',
'Arial', 'FontSize', 14 );
h= gca;
set( h, 'LineWidth', 2 );
legend( 'C_1', 'C_2', 'C_t' );

else
%
% Core impedance Rgeo < Ro
%
fgeo= sqrt(flow*fhigh);
wgeo= 2*pi*fgeo*1e6;

Leff= Rgeo/(sqrt(2)*pi*Bgeo*1e6);
Lc= Rgeo/wgeo;
Lr= Leff - Lc;

Ctgeo= 1/(Leff*wgeo^2);
%
% Look at values at flow, fgeo, and fhigh
%
wlow= 2*pi*flow*1e6;
whigh= 2*pi*fhigh*1e6;
wgeo= sqrt(wlow*whigh);

[C1xlow, C2xlow]= C12forLowZ(wlow);
[C1xgeo, C2xgeo]= C12forLowZ(wgeo);
[C1xhigh, C2xhigh]= C12forLowZ(whigh);

disp( 'Inductance Tee:' );
disp( num2str( Lr*1e9, 'Lr (nH) = %15.5f' ) );
disp( num2str( Lc*1e9, 'Lc (nH) = %15.5f' ) );
disp( ' ' );
disp( 'Inductance Pi:' );
[Lpi1, Lpi2, Lpi3]= Ltee2pi( Lr, Lc, Lr );
disp( num2str( Lpi1*1e9, 'Lr(nH) = %15.5f' ) );
disp( num2str( Lpi2*1e9, 'Lc(nH) = %15.5f' ) );

```

```

disp( ' ' );
disp( 'Freq, MHz      C1, pF      C2, pF      ' );
disp( '-----' );
disp( [num2str( flow, '%8.2f' ), ' ',
num2str(C1xlow*1e12, '%8.2f'), ' ', num2str(C2xlow*1e12, '%8.2f')
] );
disp( [num2str( fgeo, '%8.2f' ), ' ',
num2str(C1xgeo*1e12, '%8.2f'), ' ', num2str(C2xgeo*1e12, '%8.2f')
] );
disp( [num2str( fhigh, '%8.2f' ), ' ',
num2str(C1xhigh*1e12, '%8.2f'), ' ', num2str(C2xhigh*1e12, '%8.2f')
] );

fig1= figure(1);
clf;
axes( 'FontName', 'Arial', 'FontSize', 12 );

Npts= 256;
ii=1:Npts;
fswp= flow-3*Bgeo + (fhigh-flow+6*Bgeo)*(ii-1)/Npts;
[gaindB]= sweepLowZnet( fswp, Lr, Lc, C1xlow, C2xlow );
p1= plot( fswp, gaindB, 'r' );
set( p1, 'LineWidth', 2 );
hold on

[gaindB]= sweepLowZnet( fswp, Lr, Lc, C1xgeo, C2xgeo );
p1= plot( fswp, gaindB, 'k--' );
set( p1, 'LineWidth', 2 );
hold on

[gaindB]= sweepLowZnet( fswp, Lr, Lc, C1xhigh, C2xhigh );
p1= plot( fswp, gaindB, 'm:' );
set( p1, 'LineWidth', 2 );
hold on

grid on
xlabel( 'Frequency, MHz', 'FontName', 'Arial', 'FontSize', 12 );
ylabel( 'Gain, dB', 'FontName', 'Arial', 'FontSize', 12 );
title( 'Low-Z Filter Response', 'FontName', 'Arial', 'FontSize', 14
);
h= gca;
set( h, 'LineWidth', 2 );

%
% Plot tuning capacitances versus frequency
%
Np= 64;
jk=1:Np;
fswp= ( flow + (fhigh-flow)*(jk-1)/(Np-1) );
fgeo= sqrt(flow*fhigh);
for jk=1:Np
    [C1y, C2y]= C12forLowZ(2*pi*fswp(jk)*1e6);
    C1p(jk)= C1y*1e12;
    C2p(jk)= C2y*1e12;
    Ctp(jk)= (fgeo/fswp(jk))^2 * Ctgeo * 1e12;
end

figure(2);
clf;

```

```

axes( 'FontName', 'Arial', 'FontSize', 12 );
p1= plot( fswp, C1p, 'r' );
set( p1, 'LineWidth', 2 );
hold on
p1= plot( fswp, C2p, 'b--' );
set( p1, 'LineWidth', 2 );
hold on
p1= plot( fswp, Ctp, 'k:' );
set( p1, 'LineWidth', 2 );

grid on
xlabel( 'Frequency, MHz', 'FontName', 'Arial', 'FontSize', 12 );
ylabel( 'Capacitance, pF', 'FontName', 'Arial', 'FontSize', 12 );
title( 'Tuning Capacitances vs Filter Center Frequency', 'FontName',
'Arial', 'FontSize', 14 );
h= gca;
set( h, 'LineWidth', 2 );
legend( 'C_1', 'C_2', 'C_t' );
end

end
%=====
=

function [C1x, C2x]= C12forHighZ( w )
global Ro;
global Rgeo;
global gamma;
global flow;
global fhigh;
global Bgeo;
global pi;
global wgeo;
global Ctgeo;

Ct= (wgeo/w)^2 * Ctgeo;

C1x= (1/w/Ro)*sqrt( (wgeo/w)^gamma * (Ro/Rgeo) + (w*Ct)^2
*Ro*Rgeo*(w/wgeo)^gamma - 1);
C2x= 1/( w^2 *Ct/( (wgeo/w)^(2*gamma) * (1/Rgeo)^2 + (w*Ct)^2 ) - ...
(w*Ro)^2 *C1x/( 1 + (w*Ro*C1x)^2 ) );
end
%=====
=

function [gaindB]= sweepHighZnet( fswp, Lr, Lc, C1, C2 )
%
global Ro;

jx= sqrt(-1);
gaindB= zeros(1,length(fswp));
for ii=1:length(fswp)
ww= 2*pi*fswp(ii)*1e6;
abcd= [1 Ro; 0 1];
abcd= abcd*[ 1 0; jx*ww*C1 1] * [1 1/(jx*ww*C2); 0 1] * [1 0;
1/(jx*ww*Lr) 1 ];
abcd= abcd * [1 jx*ww*Lc; 0 1] * [1 0; 1/(jx*ww*Lr) 1] * [1
1/(jx*ww*C2); 0 1];
abcd= abcd * [1 0; jx*ww*C1 1] * [1 0; 1/Ro 1];

```

```

        gaindB(ii)= -20*log10( abs(abcd(1,1)) ) + 20*log10(2);
    end

end

%=====

=

function [C1x, C2x]= C12forLowZ( w )
global Ro;
global Rgeo;
global gamma;
global flow;
global fhigh;
global Bgeo;
global pi;
global wgeo;
global Ctgeo;

Ct= (wgeo/w)^2 * Ctgeo;
Rt= (w/wgeo)^gamma * Rgeo;

aa= -w^2 * Ro*Rt;
bb= 1/Ct;
dd= Rt/Ro;

alpha= (dd - bb^2/aa) / (1 - dd + bb^2/aa);
beta= (bb/aa)/( 1 - dd + bb^2/aa);

A= aa*alpha;
B= aa*beta+bb+bb*alpha;
C= bb*beta-1;

C1x= -B/(2*A) - sqrt( B^2 - 4*A*C)/(2*A);
C2x= alpha*C1x + beta;

end

%=====

=

function [gaindB]= sweepLowZnet( fswp, Lr, Lc, C1, C2 )
%
global Ro;

jx= sqrt(-1);
gaindB= zeros(1,length(fswp));
for ii=1:length(fswp)
    ww= 2*pi*fswp(ii)*1e6;
    abcd= [1 Ro; 0 1];
    abcd= abcd * [1 1/(jx*ww*C2); 0 1] * [1 0; jx*ww*C1 1] * [1 jx*ww*Lr;
0 1];
    abcd= abcd * [1 0; 1/(jx*ww*Lc) 1] * [1 jx*ww*Lr; 0 1] * [1 0;
jx*ww*C1 1];
    abcd= abcd * [1 1/(jx*ww*C2); 0 1] * [1 0; 1/Ro 1];
    gaindB(ii)= -20*log10( abs(abcd(1,1)) ) + 20*log10(2);
end

end

```

```
function [Lc, Lb, La]= Lpi2tee( L1, L2, L3 )
sigma= L1 + L2 + L3;
La= L2*L3/sigma;
Lb= L1*L3/sigma;
Lc= L1*L2/sigma;
end

function [L1, L2, L3]= Ltee2pi( La, Lb, Lc )
delta= La*Lb + Lb*Lc + La*Lc;
L1= delta/La;
L2= delta/Lb;
L3= delta/Lc;
end
```

Corrections

Version	Date	Comments
1.0	14 May 2017	Original
1.1	7 Jan 2017	Found that “C” and “D” had been improperly swapped in §6.1.3 §6.1.4. Corrections made 7 Jan 2018.